University of Stavanger

Faculty of Science and Technology

MASTER'S THESIS

Study program/ Specialization: Petroleum technology Drilling Technology	Spring semester, 2011 Open/~~Restricted access~~
Writer: Knut Tveitan	……Knut Tveitan…… (Writer's signature)
Faculty supervisor: Eirik Kårstad Seyed Ahmad Mirhaj Mohammadabadi External supervisor(s):	
Credits (ECTS): 30	
Key words: Torque and drag forces Horizontal section side bends New 3D simulation model Running of a completion string	Pages: ….……51…… + enclosure: ….....19……. Stavanger, ….04.06.201…. Date/year

Abstract

Deviated oil and gas wellbore sections keep getting longer. This is due to the fact that more fields are reaching their mature phase and due to the fact that the technical development allows us to. The number of platforms on new projects will be reduced when wells have longer horizontal sections.

In this aspect, the well friction is of importance. The friction forces will be of relevance when considering the tubular limitations in long horizontal wells with respect to the tubular yield strength specifications and buckling tendencies. Long horizontals increase the friction.

This leads to a need for friction prediction models, and they have existed for decades. The models have had their weaknesses, and in 2009 a 3-dimensional friction model was introduced with new features – among these the ability to include forces acting in side bends in the horizontal section of the wellbore. Mirhaj, Kårstad and Aadnøy (paper published in 2010) and Mirhaj, Fazaelizadeh, Kårstad and Aadnøy (paper published in 2010) have done work on the use of this 3-dimensional friction model.

Whereas work up to now with the 3-dimensional excel spreadsheet has been done on the drilling, hoisting and lowering operation of drill strings, this thesis mainly focuses on the hoisting and lowering of strings – one drill string and one completion string.

The correspondence between the 3-dimensional friction model and field hookload data has been examined, and whereas there was a good correspondence between prediction model and hookload data for the particular cases of both hoisting and lowering of a drill string, this was not the case for the operation of lowering a completion string. The 3-dimensional excel spreadsheet does have a feature weakness that may account for some of this discrepancy. Possible effects from surrounding fluids on the pipe in a curved wellbore were also investigated, but no connection between these forces and the reduced prediction model and field hookload data correspondence was found.

Table of contents

1 Introduction

1.1 Longer wells and the increasingly important role of friction

As the deviated sections of wellbores in the oil and gas industry keep getting longer, the friction in the wellbore plays an increasingly important role. The ability to keep torque losses and drag at a minimum can be critical to attain a successful well completion. Today the record departure from the platform is about 11km. To be able to drill wells with a long horizontal reach is in Norway important to drain old fields more efficiently, and to reduce the number of platforms on new projects.[1,2,5,10]

When entering wells with tubulars, limitations exist in both possible compressive load induced buckling and tensile failure due to one exceeding the tensile strength of the drill pipe. In connection to this, friction is in particular of interest in cases where the friction force is of a large enough magnitude to exceed the critical buckling load of the pipe – this leading to sinusoidally buckling. Is the friction force even greater, helical buckling of the string may occur and the drill string can become locked-up and drilling must seize. This is something the drilling engineers need to take into account by applying higher WOB, Torque-on-Bit or higher ROP. However, if the tensile load due to friction is high enough to reach the tensile strength of whatever pipe downhole in the wellbore, a string failure may occur.[1]

1.2 Torque and drag modeling

Because of the above, it is of interest for the industry to try to model the downhole torque and drag forces and keep them at a minimum. It is of importance to optimize the drillstring design and then avoid challenges with respect to both tubular buckling on one hand and tensile failure on the other.[3]

Friction modeling saw its beginning in 1984, when Johancsik et. al. introduced a model that is still somewhat valid within the industry. Here, it was assumed that all the torque and drag was caused by sliding friction forces from the contact between the drillstring and the wellbore. He

defines sliding friction to be a function of the normal contact force and the coefficient of friction between the contact surfaces. This is in accordance with the Coulumb friction model. This way of modeling was then put into a more mathematical form by Sheppard et. al. in 1987. Sheppard's model also included the upwards acting mud pressure and his model was using effective rather than true tension. Bending stiffness is however neglected in these models. Because of this, the two models described here are both so-called soft string models.[1,2,3,15]

After these two pioneers a whole lot of different torque and drag model nuances have been introduced throughout the years. However, many models are considering a 2D modeling of wellbore friction. If the whole well is drilled in one plane, like if for example the azimuth is considered a constant, the calculations can be accurate. But if the azimuth is changed, imagine one wanting to bypass a difficult formation during drilling, the calculations done with use of 2D will be questionable.[1,2]

Hence, it was of importance to find out how much the different bends in the wellbore contribute to friction. On this background, a new 3-dimensional friction model was developed in 2009. This model actually takes into account both inclination and azimuth in a dogleg.

1.3 This thesis

This thesis will also make use of this 3-dimensional torque and drag model and include forces acting in side bends in the horizontal section of the wellbore. It will aim be a small continuation of the work done by Mirhaj, Kårstad and Aadnøy (paper published in 2010) and Mirhaj, Fazaelizadeh, Kårstad and Aadnøy (paper published in 2010). The calculations will be done mathematically and analytically in an excel sheet and not by help from software. Hopefully can the results presented in this thesis contribute to further understanding of the functionality of this 3-dimensional analytical friction model.

This thesis will not have main focus on simulations done with data from while drilling, but rather a torque and drag analysis with respect to hoisting and lowering of strings. Whereas simulations so far have been done on drill strings, a goal for this thesis was that data could be

collected on the running of completion strings as well. This way, the applicability of the new 3D model can be discussed in relation to the lowering of a completion string, for instance with screens as a part of the lower completion.

2 Theory

2.1 Background

There are a number of reasons that can lead to excessive torque and drag. Among these are the presence of shale, key seats, tight-hole conditions, cuttings, differential sticking, and sliding friction. The mud type and properties will also impact on the friction factor, and hence the total torque and drag. Provided a good hole cleaning, the primary torque and drag source is however sliding friction. It can be appropriate to divide the torque and drag forces into these two main groups, namely sliding friction and friction associated with a no good hole cleaning.[2,5]

A computer model was developed by Johancsik et.al. to predict the torque and drag in a drill string. This model was based on the presumption that sliding friction is the major source of torque and drag in a directional wellbore. The sliding friction is calculated by multiplying a sidewall contact force by a friction coefficient.[3]

The sliding wellbore friction consists of two factors: the normal contact force and the friction between the contact surfaces. The product of these two will give the sliding friction force.[3]

The normal contact force is then consisting of contributions from several different factors. Johancsik et.al. only took into account the effect of gravity on the pipe and the effect of tension acting through curvatures in the wellbore. Other forces, such as pipe bending, stiffness, tripping speed, hydraulic effects, and piston effect on packed stabilizers in the BHA were not included in the model.[1,3]

Thus, it is appropriate to call this and the following models based on the Johancsik work for cable models, chain models or *soft-string models*. The drill string is then considered to be like a cable and forces owing to bending moments have not been included into the normal force, and thus friction. The models also do not capture stiffness.[1,2,15]

2.2 The torque and drag forces

2.2.1 Drag and buckling

The drag is the force required to move the pipe up or down axially in the hole. It is owing to the trajectory design, mud lubricity, wellbore condition tortuosity and other mechanical influences. Another “drag” is the drag owing to frictional forces and is the difference between the static weight of the drillstring and the tripped weight. There is also the issue of buckling. When tripping in, whether or no the string is going to sinusoidally or helically buckle, should be investigated. In addition to drill string design, rotation of the pipe and centralizers will work against buckling tendencies.[1,3,7,8]

To overcome drag, running of heavy-weight drill pipe in the near-vertical section can provide increased string weight. Hole cleaning and working the pipe can assist in getting the string down in extreme extended-reach profiles.[8]

2.2.2 Torque

The torque is the movement when rotating the pipe. The surface torque comprises of frictional string torque, bit torque, mechanical torques and dynamic torques. The torque owing to frictional forces is the difference between the torque applied at surface and the torque available at the bit. It is generated between the drillstring and casing/open hole, where contact loads are acting. The drillstring being in compression or tension, the drill pipe vs. hole size, dogleg severities, drill string weight and inclination will all impact on the contact load. To keep the contact load at a minimum, and then also the frictional torque, it is important to focus on lubricity, which is controlled by mud and formation properties.[1,3,7,8]

The bit torque can be minimized by focusing on bit optimization, whereas the dynamic torque should be kept at a minimum too since it can significantly impact operations. The mechanical torque is owing to cutting beds, borehole ledges and stabilizer effects. Like the other torque contributions, the mechanical torque should be kept at a minimum. It can be controlled via higher flow rates, careful rheology and string rotation. This will improve hole cleaning to minimize cutting beds. Identification of excessive stabilizer torque can be remedied by selection of equipment as undergauge stabilizers and reamers.[8]

2.2.3 Torque and drag relations

The torque and the drag are related by equation (2.1):

$$\left(\frac{T}{r}\right)^2 + F^2 = (\mu w \Delta s)^2 = F_{capacity} \tag{2.1}$$

The torque and drag are generally related to each other in the sense that a high drag force will occur together with a high torque load. However, if there is no rotation the drag forces will be much higher. Conversely, if the drill string is rotated, the drag forces are greatly reduced. This is illustrated in the figure 2.1 below.[7,10,12]

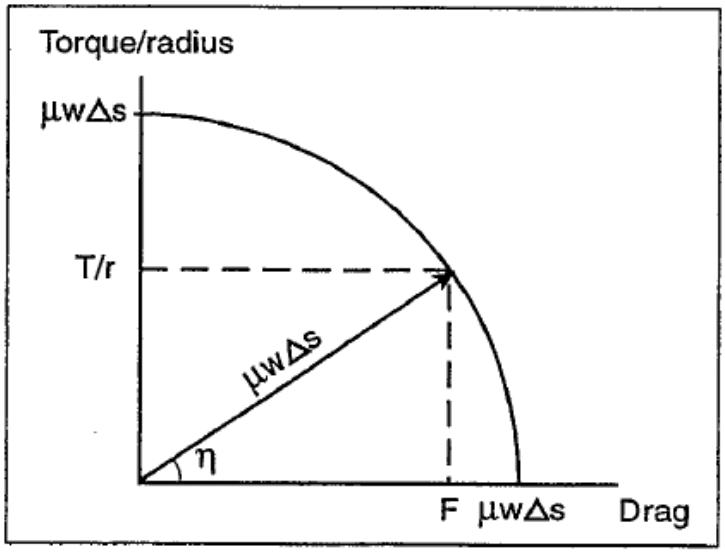

Figure 2.1: The combined friction from axial and rotational movement[10]

The above described effect can for instance be useful during installation of a liner. The combined motion when rotating the liner will reduce the axial drag and favor getting the liner down to the desired depth.[19]

2.3 The friction coefficient

2.3.1 Formula and definition

The friction coefficient is the proportionality constant from the Coulomb friction model, see equation (2.2) below:

$$F_D = \mu F_n, \tag{2.2}$$

where F_D = frictional drag force, F_n = normal force and μ = the friction coefficient. Whether the movement is axial or rotational, the result will still be the frictional resistance, F_D. Figure 2.2 below is illustrating this.[6,10]

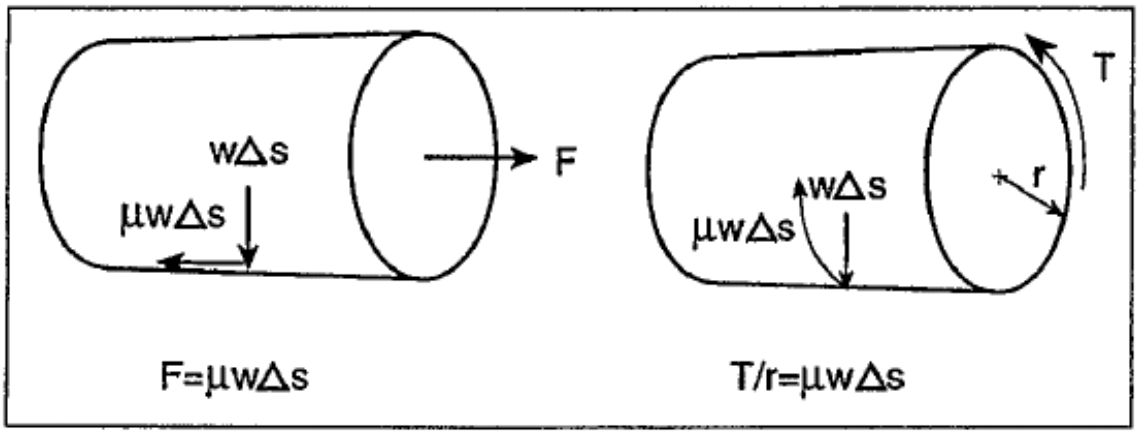

Figure 2.2: Torque and drag for a pipe[10]

The friction coefficient is really a factor lumping a bunch of other factors. These are typically mud system lubricity, cuttings, key seats, stabilizer/centralizer interaction, differential sticking, dogleg severities, hydraulic piston effect and hydrodynamic viscous forces among others. Hence, the mud type and whether one is dealing with a cased or open hole matters. For instance can a water based system friction coefficient typically vary from 0,25 to 0,4.[2,3]

2.3.2 Coefficient determination and calibration of the coefficient

Johancsik et.al. in 1984 determined their friction coefficient from field data. They used their computer model and gathered field data using novel torque and hookload indicators that were accurate, portable and easily installed. The validity of their model was confirmed by the fact that there was a good agreement between the friction coefficients calculated from different loads in the same well, in addition to good agreement from those from different wells.[3]

This kind of friction factor calibration is useful; one makes sure that one is using a friction coefficient with a high credibility. This calibration can as mentioned be achieved by comparing individually calculated friction coefficients from the same well; one calculated from the pick-up weight input data, another from the slack-off weight input data and one from

the torque data. The similarity between theses values is of interest. Also, a baseline from the same area is of importance, i.e. historical data from similar wells can tell us if we are dealing with a reliable friction coefficient value. Finally, the coefficient credibility will also depend on the accuracy of the survey data.[3]

When reverse calculating a friction coefficient from given torque and drag data, a coefficient is assumed and then iterations are performed until matching the data. Usually about six iterations are required. The friction coefficient is proportional to the torque losses. Drillstring description and a survey are required both when doing torque and drag calculations and when reverse calculating a friction coefficient.[3,5]

2.3.3 Friction coefficient to diagnose drilling problems

If one is using surface and downhole torque and WOB sensors one can on a foot-to-foot basis estimate (monitor) the friction factor. This can be useful in diagnosing drilling problems like severe doglegs and sticking zones as they occur. A sharp increase in the friction factor can then typically be seen. This way the driller is given enough time to take appropriate action to address these problems when necessary. This is of great importance, since the potential costs associated with these kinds drilling problems are high (stuck pipe, fishing jobs, lost hole etc.).[5,6]

2.3.4 Dynamic and static friction coefficient

One can also talk about a static and a dynamic friction coefficient, where the static coefficient is derived from forces required to make the initial movement of the pipe up or down or to rotate the pipe. The much more used dynamic friction factor is derived from force losses in a moving pipe.[12]

2.4 The torque and drag analysis – drillstring and well design

2.4.1 Benefits from doing a torque and drag analysis

After this, being able to predict the frictional forces acting on the pipe would be beneficial. The benefits lies in that highly deviated wells can be planned to keep the torque and drag forces at a minimum. Also, knowledge of the drillstring loadings can give us an opportunity to

choose drillstring components through a systemic approach that considers these extra forces involved in the operations.[3]

2.4.2 Drillstring design

The drillstring design is an integrated part of doing a torque and drag analysis. In this design, there are typically four criteria that are emphasized. These are:

- The rotary torque must be within what the rotary drive system and drillstring can take. There should be a safety margin as well.
- The same as above goes for the up and down drags. Downwards, no buckling can be induced. There should be a safety margin.
- Also, there should be safe thresholds for the contact forces between the tool joints and the borehole wall.
- Finally, the drillstring must not be induced to buckling along its length for the entire range of anticipated bit weights.[6]

It will the be up to the planning engineer to comply with all these criteria by varying wellbore geometry, mud system and drillstring design.[6]

2.4.3 Well design considerations

Six methods can typically be used to calculate a wellpath trajectory to reach a geological objective. These are the tangential, the average angle, the balanced tangential, the mercury, the minimum curvature and the radius of curvature method. To maximize survey accuracy, a natural choice is the demanding minimum curvature method. Even though the survey calculation method really plays a minor role in the torque and drag analysis results, the overall wellpath design is more accurate and better off using the minimum curvature method as opposed to the other methods. Figure 2.3 below shows the forces and geometries of different curved hole sections when applying the minimum curvature method.[10,16]

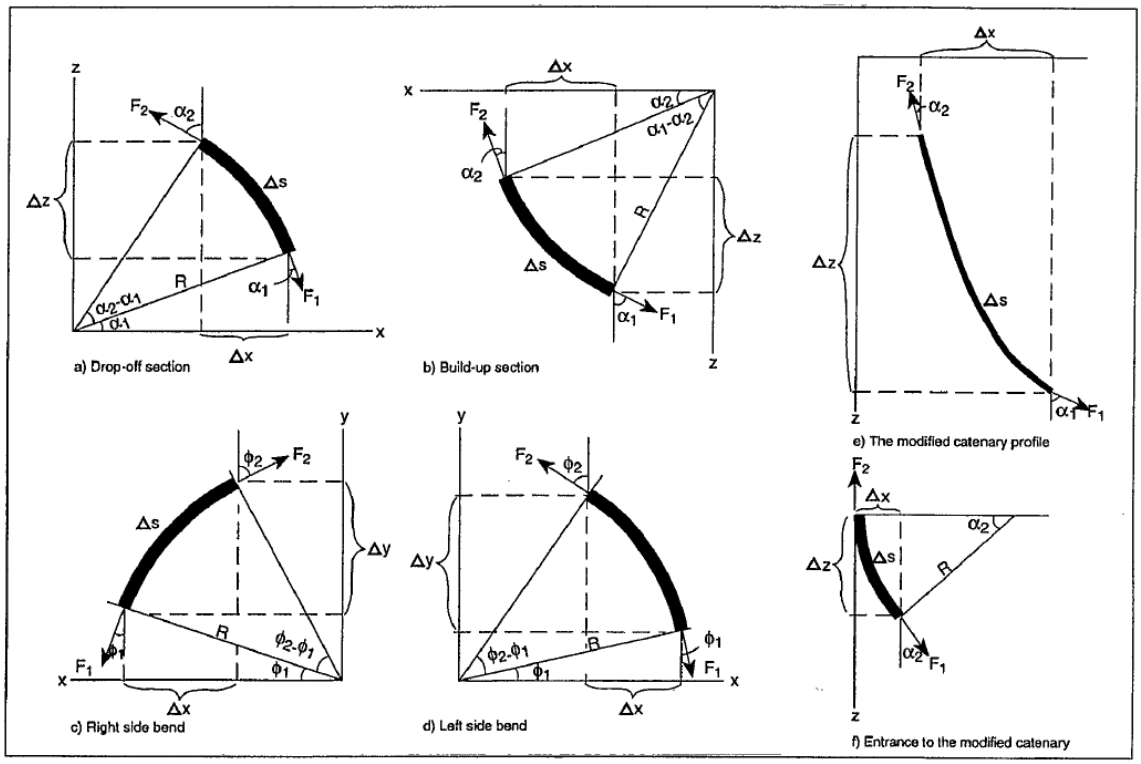

Figure 2.3: Forces and geometries of various curved hole sections[10]

Still, this method has also been shown to have weaknesses with respect to inclusion of the bending moment. The bending stresses can be discontinuous at survey points. Hence, the minimum-curvature may not always give an exact representation of a real drillstring configuration.[9,15]

In addition to wellpath design, also other issues are critical to bear in mind when planning extended-reach wells. These can typically be casing seat selection, wellbore stability and drilling mud. Next, the capabilities of the hydraulic pump system should be considered. Rig sizing and selection should also not be ignored.[13]

2.4.4 Well path design: Undersection trajectory and the catenary well profile

Sheppard et.al. found in 1987 that a deviated well with an undersection trajectory can exhibit lower torque and drag in certain circumstances than a conventional well geometry would. Undersection here has the meaning of a trajectory which is constantly building angle and lying below a conventional tangent section.[4]

Even though this undersection well may show a reduced drag, these cases demonstrate that the drill collar side forces will increase. This again can make the BHA stick more easily. Therefore, this example of reducing torque and drag (by making use of an undersection) must be used with caution. Especially is this the case where hole instability, differential sticking or poor hole cleaning is anticipated.[4]

The catenary profile was first introduced to the oil industry in 1985. This profile is sort of mimicking the shape of a hanging rope. The string is hanging like a rope in a borehole also shaped as a rope. The idea is that there potentially is "no contact at all between the drillstring and the borehole wall". Therefore there will be zero normal force, and hence no friction. This catenary curve will lead to a much longer well path than the more traditional well profiles. See figure 2.4 below for illustration of the catenary curve.[4,7,13,17]

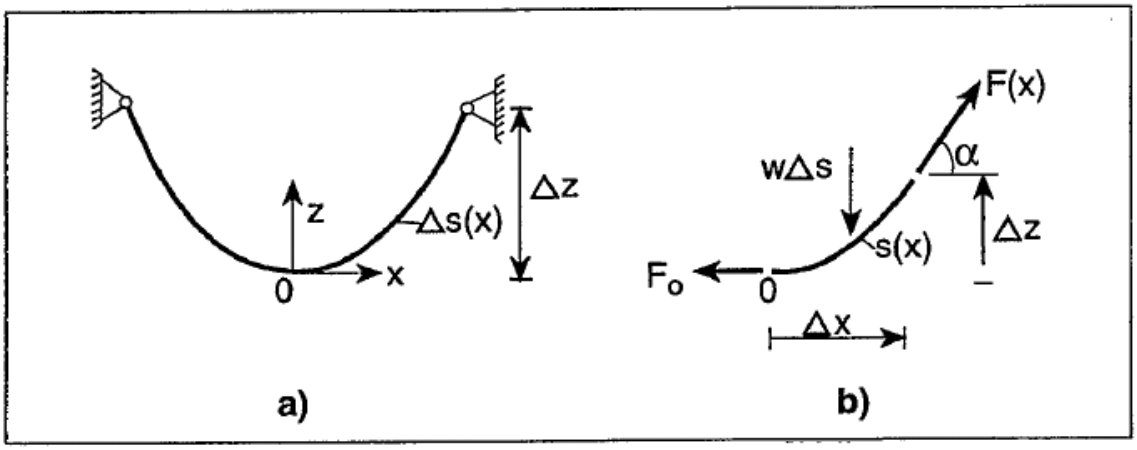

Figure 2.4: Catenary profile – the shape of a free-hanging rope[10]

However, there are some downsides associated with the catenary profile. These are mainly that there will be friction in a buildup section in the beginning of the profile, counteracting the total benefits with respect to torque and drag overall (onshore this friction contribution can be reduced by the use of a slant rig). Secondly, the string tension must be kept accurately controlled and there are only a few operations that are suited for harvesting the benefits from this profile with regards to reduction of torque and drag losses. Also, the profile requires a horizontal end condition at the bottom (see figure above). To go around these catenary profile challenges, a "modified catenary string model" has been introduced.[13,17]

2.5 Torque and drag measurements and following calculations

2.5.1 Measurement of torque and drag

The drag is found by use of a weight indicator on the rig. It measures the WOB, the drag and over-pull forces. This is usually an accurate and repeatable method. If you are inaccurate when accounting for the weight of the traveling equipment (which needs to be subtracted), errors can be induced. To produce a calibration curve, information from the weight indicator is plotted with data from a weight indicator calibration sub.[3]

The torque is it on the other hand much more difficult to get reliable readings on. For use portable torque meters exist, these are placed between the rotary table and the drive bushing. The apparatus provides oscillating values; an average must be used.[3]

2.5.2 Basic principles behind the calculations

Once all necessary information is at hand, being drillstring description, survey data and friction coefficient, the calculations can begin. The first step will be to calculate the normal force. The magnitude of this force is given by equation (2.3):

$$F_n = \left[\left(F_t \Delta\alpha \sin\theta \right)^2 + \left(F_t \Delta\theta + W \sin \right)^2 \right]^{0,5} \tag{2.3}$$

This equation then leads to equations for increments from tension (2.4) and torsion (2.5):

$$F_t = W \cos\theta \pm \mu F_n \tag{2.4}$$

$$\Delta M = \mu F_n r \tag{2.5}$$

The friction contribution from each geometrical section from bottom up can be calculated. The result will be a friction at surface due to contact friction from along the wellbore. The total friction will actually be a sum of the surface friction and friction due to drilling fluid and cuttings friction. Today, it is however common practice to use an overall friction coefficient, because equations for mud friction is yet not derived. To get accuracy in the results, it is also important to keep the elements short, since calculations using longer intervals will induce small errors due to second-order terms from the equations above.[2,3,10]

2.5.3 How to perform the calculations

Having an overall friction coefficient at hand the calculations of torque and drag can start from the bottom of the drillstring and commence upwards. Which formulas to make use of to calculate the forces will depend on the well design. For a typical well with a build-and-hold profile, the first force that will be calculated is the F_1, the bit force, at the bottom. F_2 will be the force of the BHA section added to the F_1. F_3 is the force of the sail section added to the F_2. F_4 is the force of the Kick-off section plus the F_3. F_5 is the force of the vertical section, with F_4 added to it. The formulas for the pulling the string, lowering the string and drilling are all different. See figure 2.5 below for examples of build-and-hold profiles.[17]

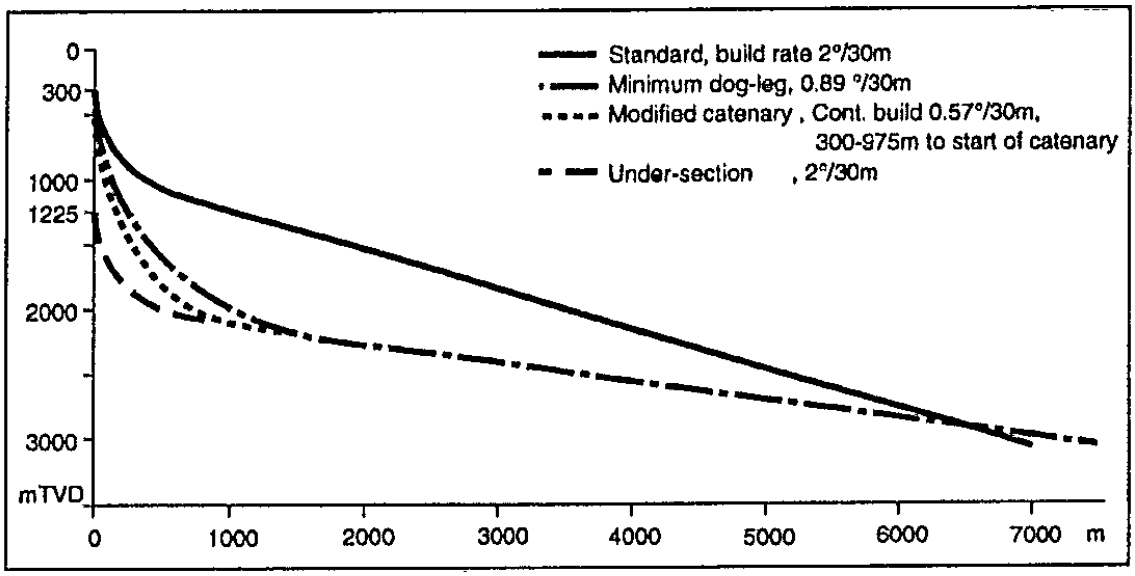

Figure 2.5: Different build-and-hold profiles[10]

2.5.3 The different analysis modes

The typical scenarios of interest to simulate against torque and drag forces are when drilling, when tripping in and when tripping out. The different calculations can also be done to simulate how the force balances will interact when running a completion string. Will it for example possible to reach TD with the current string and string configuration?[1,3,8,11]

2.6 Summary of development and papers 1984-2010

1984: Johancsik presents the pioneer friction analysis model
1987: Sheppard takes the Johancsik model into differential form and included buoyancy effects. I.e. he used effective tension instead of true tension.
1988: Lesage et.al. separates the friction factor for drilling and wiper trips, and sliding friction factor for downhole motor drilling and tripping in and out without rotation.
1994: Aarrestad discusses the benefits from using the catenary well profile. This is a continuation of Sheppard's proposal introduced in 1987.
1998: Payne et.al. discuss buckling, cuttings bed and wellbore trajectory relations in the torque and drag analysis.
2006: Aadnoy derives the mathematical equations for the catenary well profile and applies them on a field case study on an ultralong well, comparing the results to the ones obtained from a conventional well.
2008: Aadnoy develops a new generalized model for torque and drag, a model accounting for torque and drag in bends.
2010: Mirhaj et.al. study a 3-dimensional model developed in 2009, to examine the effects on friction when including bends in the horizontal section of an ERD well.[2,10]

2.7 More on the 3-dimensional analytical friction model

2.7.1 The 3-dimensional analytical friction model

In 2009 a new 3-dimensional friction model was developed. This model also includes potential azimuth changes along the wellpath, in contradiction to the other models based on Johancsik and Sheppard's early work. The azimuth changes can for instance arise from troublesome formations that need to be bypassed. General belief is that side bends like these do make a contribution to the total friction in the well.[1]

A case study from 2010 by Mirhaj, Kaarstad and Aadnoy shows that during hoisting, a weightless BHA is not necessarily the case through a side bend. This is because compression rather than tension is dominant and many stabilizers will add to stiffness. The stabilizers add to friction and the result is that the soft-string model will be less suited for the calculation,

since it does not take either stiffness or bending into account. When weight is dominant the pipe will lie against the low-side of the borehole, whereas it will lie against the sidewall when tension is. See figure 2.6 below. Therefore, it is important to find out if it is weight or tension which is the dominating force in the horizontal section of the wellbore. This can be done by assuming equal the expression for horizontal friction when the pipe is assumed weightless and the expression for when it is not, and then solving for a critical force value:

$$F = \frac{W * L * \sin a}{2 * \sin\left(\frac{q}{2}\right)} \tag{2.6}$$

Equation (2.6) is then introduced to the friction model to improve the underprediction of BHA weight in the horizontal section when using the friction model.[1,17]

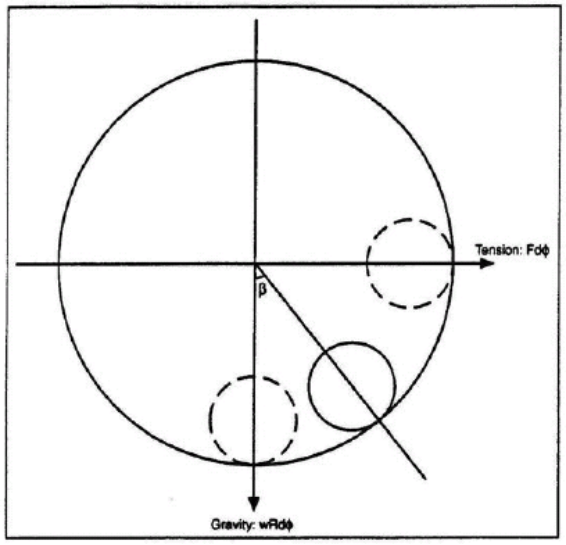

Figure 2.6: Drillpipe position in the borehole for a side bend[1,17]

The authors of this modified friction model found that the modified model matched a given friction factor in their case study when there was presence of side bends in the horizontal section. This was both when simulating tripping out and tripping in. The Johancsik model over-predicted the friction in this particular case. The drilling simulation showed, however, relatively consistent results irrespective of friction model choice. The drilling friction factor was however in this particular case small: 0,01.[1]

The authors of this paper also found that other effects could have considerable effect on friction. These were the tripping speed, hydraulic effects, a piston effect on packed stabilizers in BHA and the already mentioned stiffness. The effect of these parameters should be investigated in future studies.[1]

2.7.2 Formula overview

2.7.2.1 Wellbore orientation formulas

In addition to the measured azimuth and inclination, the dogleg and a dogleg severity are computed. The dogleg is an absolute change of direction, whereas the dogleg severity is the derivative of the dogleg. The respective formulas (2.7) and (2.9) are shown below.[19]

$$DL[\deg rees] = \frac{180}{\pi}\left|\theta(rad)\right| \tag{2.7}$$

where:

$$\cos\theta = \sin\alpha_1 \sin\alpha_2 \cos(\phi_1 - \phi_2) + \cos\alpha_1 \cos\alpha \tag{2.8}$$

$$DLS[\deg rees] = \frac{DL}{\Delta L(m)}\left(\frac{\deg rees}{m}\right) \tag{2.9}$$

2.7.2.2 String tension formulas

The effective string weight of the pipe is the pipe weight multiplied with a buoyancy factor. The buoyancy factor formula is determined by one out of two formulae, depending on if there is the same fluid inside and outside of the pipe or not. Below are the two buoyancy formulas (2.10) and (2.11) shown.[19]

$$\beta = 1 - \frac{\rho_0 A_0 - \rho_i A_i}{\rho_{pipe}(A_0 - A_i)} \tag{2.10}$$

$$\beta = 1 - \frac{r_0}{r_{pipe}} \tag{2.11}$$

The static string weight needs to be found, and will be done so by multiplication of the buoyed pipe weight with the projected vertical height of the well. Alternatively, it can be found via setting the friction factor equal to zero in the friction equation defined in the subchapter below.[19]

2.7.2.3 The 3-dimensional friction model formulas

This chapter will deal with calculation of hookloads during hoisting and lowering operations for a wellbore string, and torque calculations. The equation sets are of two types, one for straight sections and the other one for sections with an arbitrary well orientation.[19]

For *drag in an inclined wellbore section without pipe rotation*, typically pipe tension does not contribute to normal pipe force, and then friction. The sections are weight dominated. See below for this formula (2.12).[19]

$$F_2 = F_1 + \beta \Delta L w \{\cos\alpha \pm \mu \sin\alpha\}, \tag{2.12}$$

where "+" means hoisting and "–" means lowering of the pipe.

Secondly, below the *torque formula (2.13) for straight inclined wellbore sections without axial pipe motion.*[19]

$$T = \mu r \beta w \Delta L \sin\alpha \tag{2.13}$$

Thirdly, below is the formula (2.14) for the *drag in curved wellbore sections without pipe rotation*. In these curved borehole sections, axial pipe loading is the primary contributor to the axial pipe loading and the process is tension dominated. The pipe will be assumed weightless and weight will be added at the end.[19]

$$F_2 = F_1 e^{\pm\mu|\theta_2 - \theta_1|} + \beta w \Delta L \left\{ \frac{\sin\alpha_2 - \sin\alpha_1}{\alpha_2 - \alpha_1} \right\} \tag{2.14}$$

Then the formula (2.15) for *torque for curved wellbore sections without axial motion* is up next:[19]

$$T = \mu r N = \mu r F_1 |\theta_2 - \theta_1| \tag{2.15}$$

After this, friction calculations can be done by dividing the wellbore into straight and curved parts. The forces and torques are, as previously described in chapter 2.5.2, calculated from bottom and upwards.[19]

There will however be necessary with some modifications to the formulas when dealing with *combined axial and rotational motions.* Below are the respective formulas (2.16) and (2.17) for straight sections.[19]

$$F_2 = F_1 + \beta w \Delta L \cos\alpha \pm \mu \beta w \Delta L \sin\alpha \sin\gamma \tag{2.16}$$

$$T = r\mu\beta w \Delta L \sin\alpha \cos\gamma \ , \tag{2.17}$$

where

$$\gamma = \tan^{-1}\left(\frac{V_h}{V_r}\right) = \tan^{-1}\left(\frac{60 V_h \left(\frac{m}{s}\right)}{2\pi N_r (rpm) r(m)}\right) \tag{2.18}$$

Following this, the formulas (2.19) and (2.20) for curved pipe sections are found below. The formula for γ will correspond to the one for γ above.[19]

$$F_2 = F_1 + F_1\left(e^{\pm\mu|\theta_2-\theta_1|} - 1\right)\sin\gamma + \beta w \Delta L\left\{\frac{\sin\alpha_2 - \sin\alpha_1}{\alpha_2 - \alpha_1}\right\} \tag{2.19}$$

$$T = \mu r N = \mu r F_1 |\theta_2 - \theta_1| \cos\gamma \tag{2.20}$$

The summation sign sigma, Σ, can/should be included in the formulas to account for any changes in wellbore geometry or size.[20]

2.8 Effective force

2.8.1 Effective pressure forces in a curved wellbore

When including effects of the surrounding fluids on the pipe, a term effective force is used. There has been written many papers on this subject, but effective force in general not really paid much attention in the oil industry. The same goes for the inclusion of these effects in torque and drag modeling.[1,21]

Klinkenberg and Lubinski developed the earliest equations on the phenomenon half a century ago, but here the equations (2.21) and (2.22) below determining the fluid side force will be utilized:[21]

$$\vec{w}_{st} = [p_o A_o - p_i A_i]\vec{kn} \tag{2.21}$$

where:

$$k = \frac{1}{R} \tag{2.22}$$

The pressure loads will depend on the wellbore radius of curvature, R, see equations above.[21]

2.8.2 The radius, R, in a curved wellbore

The radius, R, in a curved wellbore can be found from equation (2.23) below:[1]

$$R = \frac{18000}{\pi f} \tag{2.23}$$

where f is in degrees per 100 feet. The degrees per 100 feet, now called DLS, can be found from equation (2.24):[1]

$$DLS = 100\frac{f}{L} \tag{2.24}$$

where f this time around is the dogleg angle in degrees. And this dogleg angle in degrees can ultimately be found from equation (2.25):[1]

$$f = \cos^{-1}\{\cos(a_2 - a_1) - \sin a_1 \sin a_2 [1 - \cos(b_2 - b_1)]\} \tag{2.25}$$

The dogleg angle in degrees is a standard occurring column in well survey material.

2.9 Some last comments on buckling, performing calculations and HWDP

Tubular buckling models can typically be divided into two groups or schools depending on who the authors behind the models would be. They differ in terms of scope of application and impact on modeling. The two are called the conservative and the extended buckling mode. The main difference between them is the size of the indices for modifiers to stiffness and the normal force terms; these are higher for the extended buckling mode.[9]

When simulating it is important to look at different sections of a wellbore individually, to simulate in the different drilling modes (rotary drilling, slide drilling and tripping), to find the maximum WOB without buckling the pipe, find the tripping capabilities and also the frictional tolerances. The most important contributors can be said to be the WOB and the friction factors.[9]

HWDP typically has two functions. They can add string weight, but they can also withstand compressive loads because of their mechanical properties. They have the greatest impact on adding weight in the vertical well section.[9]

All torque and drag simulations can be done either analytically "by hand" by use of an excel-sheet, or by using software models. Different software models have existed since the 1990s.[1,14]

3 Experimental methods

3.1 Equipment

The following equipment was used for this thesis:

- An excel spreadsheet tool with three different torque and drag prediction models
- Field data from a North Sea well provided from BakerHughes INTEQ
- Field data from three North Sea wells on the same field provided from an operator on the Norwegian continental shelf

3.2 Input field data to the excel spreadsheet

3.2.1 The data material and how to get hold of it – completion string vs. drilling string data

To begin with, a previous University of Stavanger source in BakerHughes INTEQ was contacted to access field data. The plan for this thesis was to investigate the running of a completion string and see how the new 3D model would predict the hookloads and torque and drag losses.

The process of collecting field data however proved to be a long and demanding process. The material received was either incomplete, a mixture of material stemming from different wells or material that simply had been used in a previous analysis. After many mails and phone calls back and forth, a complete data set was finally collected. This data set was from a drilling operation in a long horizontal North Sea well. I.e. the material was containing drill string data, rather than completion string data. This data set will be denoted well data set A.

On this background, a wider source material search was initiated. Three operating companies were contacted, and after a while one of these contacts responded and gave access to data from three North Sea wells containing completion string data. The well type of these three wells was also horizontal; the length of the horizontal section was however shorter than that of the extremely horizontal well in data set A.

The material at hand for the four wells was now survey, string info and an excel sheet with offshore recorded data like measured depth, hookloads and torque. Well data set A also had other parameters like for example ROP and WOB, mud flow in and mud flow out.

3.2.2 Which input parameters to put into the experimental excel tool

Once possessing the field data and the excel experiment tool, input parameters were to be incorporated into the excel spreadsheet. The input parameters to be used were the following single values:

- *mud weight*, MW [s.g.]; collected from the column "mud density in" among the field data for the single horizontal well, and from the completion brine weight for the other three wells
- *friction factor*, μ ; arbitrary value to be used in different trials to decide on one probable friction factor that was to be used in the analysis
- "*tension limit*", F [kN]; see chapter 3.3.3 for determination of this parameter
- *block weight*, [tons]; found from explicit question to the rig
- *drill string data*; being unit weight $\left[\frac{kN}{m}\right]$ with length [m] for different string sections

The drill string data will be further elaborated on below.

Into columns, the following data were needed:

- *measured depth*, [m]; found from survey
- *radius* of drillstring, [m]; found from string report and running list
- *azimuth*, (converted from degrees to radians); found from survey
- *inclination*, (converted from degrees to radians), found from survey
- *true vertical depth*, [m]; found from survey
- *recorded hookloads*, [tons]; found in recorded offshore drilling data ASCI file

Figure 3.1 below is presenting a clip from one of the 3D excel tool spreadsheets and is showing whereabouts of the parameters described above.

	B	C	D	E	F	G	H	I	J	K	L	M	R	S	T	U
1													DRAG			
2			MW	1,12	Sg	Edit drill string data			Calculate hook loads							
3			μ	0,2							New					
4			Tension limit	90							3D Model		Texas Model		Exxon Model	
5	Depth(m)	w(kN/m)	w(kN/m)	r(m)	μ	α(rad)	φ(rad)	TVD(m)	θ(rad)	ΔL (m)	Hoisting (kl	owering(kl	Hoisting	Lowering	Hoisting	Lowering
6																
7	0,00	0,3064	0,262718624	0,092075	0,2	0,00	0,00	0,00	0	3	742,3628931	257,30849	762,952	229,3067	824,6753	60,03945
8	3,00	0,3064	0,262718624	0,092075	0,2	0,00	0,00	3,00	0	358,2	741,5747372	256,52034	762,163	228,5185	823,8871	59,25129
9	361,20	0,3064	0,262718624	0,092075	0,2	0,00	0,00	361,20	0	16,8	647,4689261	162,41453	668,058	134,4127	729,7813	-34,8545
10	378,00	0,3064	0,262718624	0,092075	0,2	0,01	3,73	378,00	0,0096	8	643,0552532	158,00085	662,368	130,2534	722,4337	-39,1072
11	386,00	0,3064	0,262718624	0,092075	0,2	0,01	3,79	386,00	0,00267	10	640,949566	155,90324	660,262	128,1558	719,9442	-41,1903
12	396,00	0,3064	0,262718624	0,092075	0,2	0,00	4,60	396,00	0,00506	9	638,3187756	153,27978	657,632	125,5323	716,5646	-43,7727
13	405,00	0,3064	0,262718624	0,092075	0,2	0,01	4,53	405,00	0,00404	12	635,9520252	150,91765	655,265	123,1702	713,6261	-46,0965
14	417,00	0,3064	0,262718624	0,092075	0,2	0,01	3,51	417,00	0,00977	18	632,7939143	147,77077	652,107	120,0233	709,0238	-49,1471
15	435,00	0,3064	0,262718624	0,092075	0,2	0,00	0,78	435,00	0,01327	26	628,0550217	143,05234	648,435	115,4903	701,4689	-53,6624
16	461,00	0,3064	0,262718624	0,092075	0,2	0,01	3,00	461,00	0,01448	24	621,2207843	136,22526	640,298	108,8908	691,8985	-60,2483
17	485,00	0,3064	0,262718624	0,092075	0,2	0,03	3,28	484,99	0,01572	29	614,8999826	129,93659	632,093	102,9176	683,4511	-66,3181
18	514,00	0,3064	0,262718624	0,092075	0,2	0,05	3,21	513,97	0,02597	30	607,2420248	122,36266	621,21	95,86193	672,4053	-73,4874
19	544,00	0,3064	0,262718624	0,092075	0,2	0,10	3,31	543,88	0,04595	28	599,2875576	114,57649	607,718	88,93005	658,605	-80,4871
20	572,00	0,3064	0,262718624	0,092075	0,2	0,14	3,32	571,67	0,04421	29	591,8222001	107,40133	594,985	82,5338	645,7702	-86,8445
21	601,00	0,3064	0,262718624	0,092075	0,2	0,17	3,23	600,32	0,03008	29	584,0639935	100,07726	584,184	75,63746	634,6243	-93,5937
22	630,00	0,3064	0,262718624	0,092075	0,2	0,20	3,24	628,83	0,03169	30	576,2974143	92,823111	572,797	68,86324	623,462	-100,169
23	660,00	0,3064	0,262718624	0,092075	0,2	0,23	3,18	658,12	0,0366	29	568,2598097	85,413499	560,963	61,92676	611,5999	-106,761
24	689,00	0,3064	0,262718624	0,092075	0,2	0,28	3,18	686,17	0,04399	28	560,4954052	78,356907	548,384	55,43093	599,3433	-112,752
25	717,00	0,3064	0,262718624	0,092075	0,2	0,33	3,21	712,87	0,05414	25	553,0181906	71,688273	535,212	49,38385	586,412	-118,053
26	742,00	0,3064	0,262718624	0,092075	0,2	0,35	3,24	736,45	0,01703	8	540,9338499	66,206011	527,171	43,74166	578,5659	-123,439
27	750,00	0,3064	0,262718624	0,092075	0,2	0,37	3,18	743,95	0,03296	43	538,8138339	64,37044	522,368	42,13727	572,9335	-124,467
28	793,00	0,3064	0,262718624	0,092075	0,2	0,43	3,19	783,56	0,05621	29,7	527,4661481	54,660525	505,403	32,97599	557,1382	-132,509
29	822,70	0,3064	0,262718624	0,092075	0,2	0,47	3,16	810,36	0,03969	28,7	514,6096989	48,160203	493,932	26,81421	546,4023	-137,799
30	851,40	0,3064	0,262718624	0,092075	0,2	0,50	3,09	835,80	0,04378	39,2	507,1943034	42,097607	483,463	20,96182	535,5094	-142,661
31	890,60	0,3064	0,262718624	0,092075	0,2	0,56	3,00	869,69	0,07377	18,7	497,1598504	34,027511	468,053	13,24651	519,7218	-148,488
32	909,30	0,3064	0,262718624	0,092075	0,2	0,58	3,02	885,47	0,02436	30,6	485,7936646	30,326486	461,351	9,671117	513,5373	-151,399
33	939,90	0,3064	0,262718624	0,092075	0,2	0,53	3,09	911,47	0,05595	28,1	478,1805102	24,468949	457,65	3,722684	500,425	-157,006
34	968,00	0,3064	0,262718624	0,092075	0,2	0,50	3,15	935,87	0,04326	28,3	466,5206048	18,262066	453,244	-1,96722	489,241	-162,38
35	996,30	0,3064	0,262718624	0,092075	0,2	0,47	3,22	960,87	0,04413	28,7	459,2917475	12,469115	448,878	-7,88934	477,9202	-167,865
36	1025,00	0,3064	0,262718624	0,092075	0,2	0,45	3,34	986,60	0,05811	32,3	451,8896429	6,4371886	443,665	-14,0504	465,4297	-172,799
37	1057,30	0,3064	0,262718624	0,092075	0,2	0,43	3,47	1015,85	0,05775	29,1	439,0746986	-1,2598861	436,664	-21,08	452,2754	-178,495
38	1086,40	0,3064	0,262718624	0,092075	0,2	0,41	3,60	1042,40	0,05507	29,1	427,1387898	-8,3292638	430,506	-27,5195	440,2243	-183,541
39	1115,50	0,3064	0,262718624	0,092075	0,2	0,42	3,75	1069,00	0,06304	28,9	415,5520691	-15,483796	422,089	-33,9481	427,8986	-187,984
40	1144,40	0,3064	0,262718624	0,092075	0,2	0,44	3,89	1095,28	0,06129	29	403,5290974	-22,670689	413,543	-40,3171	415,9803	-192,326

Figure 3.1: Facsimile of a part of the excel tool used in these thesis experiments

3.2.3 The drill string data

The drill string data button needs to be hit to fill in drill string info, see figure 3.2 below. The drill string info will then be categorized into three parts. Hence, all drill string info will need to sort under “BHA”, “Lower drill pipe” or “Upper drill pipe”. After hitting “OK”, all this string info is transferred into every excel calculation row.

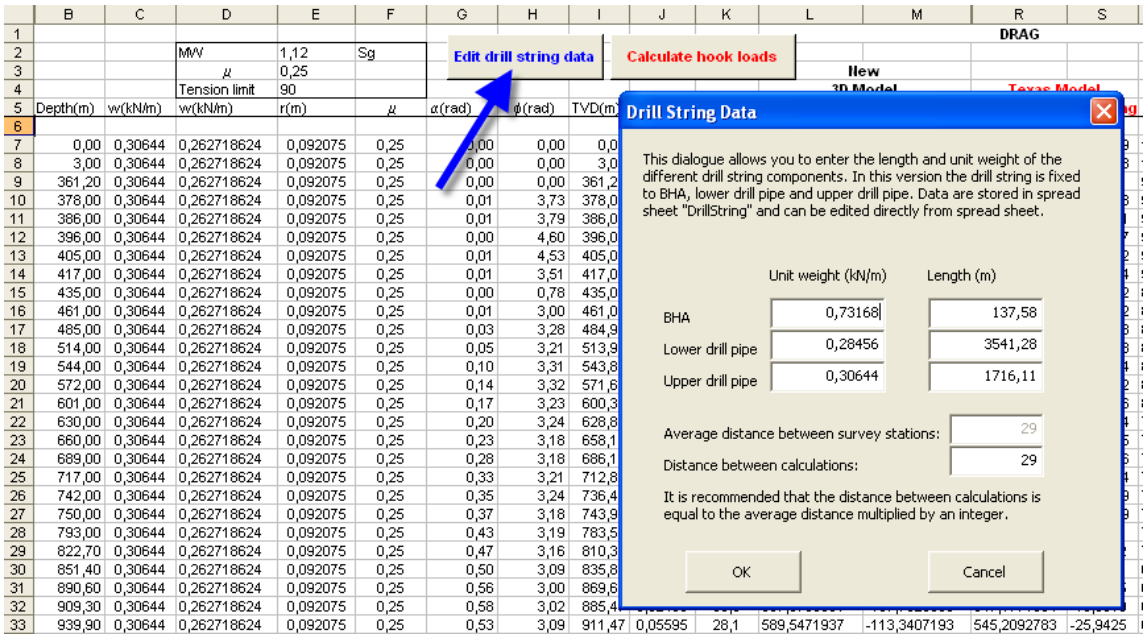

Figure 3.2: Drill string data button and pop-up box

3.3 The spreadsheet functionality

3.3.1 The experimental tool: an excel sheet

The tool that was used in this experiment was as previously stated an excel sheet containing formulas to predict torque and drag from three different frictional models. The spreadsheet was developed in 2009 and has been case studied in 2010 by Mirhaj, Kaarstad and Aadnoy.

3.3.2 The three frictional models

The Johancsik model from 1984 was the first one of the prediction models, a model still applicable for torque and drag simulators in the oil and gas industry. The Johancsik model is in this experiment and excel spreadsheet called the Exxon model.

The second model was originally a 2D-model. It has however been modified by Mirhaj, Fazaelizadeh, Kaarstad and Aadnøy, the authors of “New Aspects of Torque-and-Drag Modeling in Extended-Reach Wells”, into a 3-D model in order to make it applicable for side bends as well as build/drop sections. It is in the experimental spreadsheet called the modified Texas A & M model.

The last T & D model to be applied is the new analytic fully 3-dimensional torque and drag model published by Aadnoy, Fazaeli and Hareland in 2009. This model incorporates many new features. It introduces dog-leg severity for build/drop and side bend sections.

3.3.3 What's to be calculated?

3.3.3.1 To be calculated in advance: the tension limit

The tension limit has to do with equation (2.6) presented in the theory chapter. The equation is applied to determine whether the drillstring is tension dominated or weight dominated in the horizontal section.

$$F = \frac{W * L * \sin a}{2 * \sin\left(\frac{q}{2}\right)}$$

First the largest value for the azimuth, q, is found among the data material. Then the corresponding values for the other unknowns in the formula are used from the same well position as q. Then the formula is solved with respect to the force F, and this value is then entered into the excel document. This tension limit value is primarily relevant for the torque calculations.

3.3.3.2 Calculations done by the excel tool: Hookloads, torque, static weight

Once all the input data has been entered into the excel document, one is set to hit the "Calculate hook loads" button. See red arrow in figure 3.2 below for whereabouts of this button in facsimile.

	B	C	D	E	F	G	H	I	J	K	L	M	R	S	T	U
1													DRAG			
2			MW	1,12	Sg	Edit drill string data			Calculate hook loads							
3			μ	0,25							New					
4			Tension limit	90							3D Model		Texas Model		Exxon Model	
5	Depth(m)	w(kN/m)	w(kN/m)	r(m)	μ	α(rad)	φ(rad)	TVD(m)	θ(rad)	ΔL (m)	Hoisting (kll)	Lowering(kll)	Hoisting	Lowering	Hoisting	Lowering
6																
7	0,00	0,30644	0,262718624	0,092075	0,25	0,00	0,00	0,00	0	3	865,1806581	117,9703432	880,4216503	200,8009	1022,547	-128,267
8	3,00	0,30644	0,262718624	0,092075	0,25	0,00	0,00	3,00	0	358,2	864,3925022	117,1821874	879,6334944	200,0128	1021,759	-129,055
9	361,20	0,30644	0,262718624	0,092075	0,25	0,00	0,00	361,20	0	16,8	770,286691	23,07637616	785,5276832	105,907	927,6529	-223,161
10	378,00	0,30644	0,262718624	0,092075	0,25	0,01	3,73	378,00	0,0096	8	765,8730181	18,66270328	779,2387551	101,7428	918,5754	-226,422

Figure 3.3: Whereabouts of the "run" or "enter" button in the excel tool

After the button has been hit, some seconds will pass as all the calculations are being performed. When ready, columns will be filled with the calculated values on each measured depth calculating point, like they already have been in figure 3.2 above (at four depth points).

The columns are showing calculated hookloads from the use of the three different friction models. Two pre-programmed macros will have prepared the hookloads to be simulated when both lowering the string and hoisting the string. Hence the drag is shown in six columns, during hoisting and lowering for all three friction models. The same goes for the torque, which then will provide twelve columns total.

Finally, also the static string weight has been calculated; thus giving us first and foremost six drag columns, six torque columns and one static string weight column.

3.3.4 The Plots

3.3.4.1 Plotting of horizontal displacement vs. TVD and azimuth/inclination vs. MD

To more clearly see what kind of a well is being dealt with, a plot of horizontal displacement vs. true vertical depth is made from the survey data. This plot will show whereabouts of KOP, build section or sections and illustrate length of the horizontal section. The plot can be useful in the discussion part to help understanding different relations amongst the data material, maybe in particular since the applicability of the 3D model is thought to work best throughout long horizontals. The plot is to be found under the well info in chapter 4.3. See figure 3.4 for an example on such a plot below.

In the same chapter a plot of azimuth and inclination vs. measured depth is shown. This plot will demonstrate whereabouts of turns in the wellbore and also be of interest when performing the data analysis. See figure 3.5 below for an example on this kind of a plot.

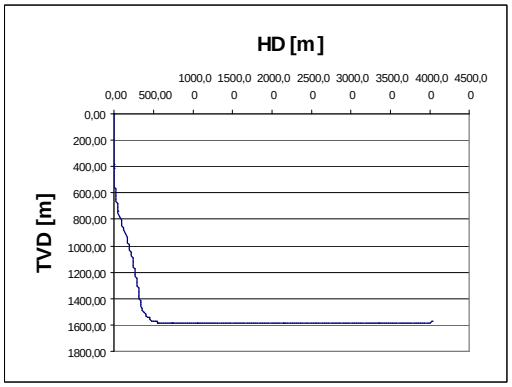

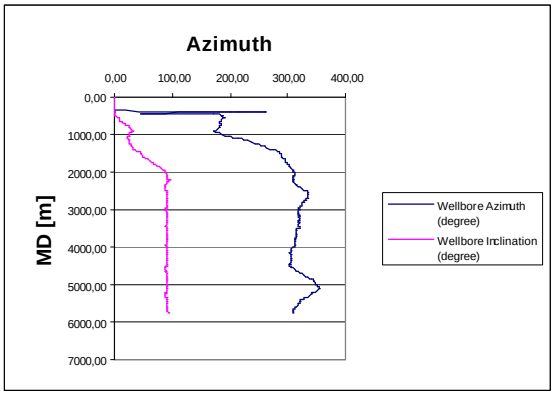

Figure 3.4 and 3.5: Examples on horizontal displacement vs. TVD and azimuth/inclination vs. MD. Here from this thesis well data set A.

3.3.4.2 Plotting of hookload results

The true field data of hookloads are several thousand measurements done during the operations in a particular well. When presented in a diagram, these measured hookloads are plotted against measured depth and shown as a bunch of black dots in the diagram. The calculated hookload values from the three different frictional models are on the other hand done approximately every 50 meter of measured depth. These values are plotted into the same diagram as the true field data sample dots, and three trend-lines are drawn between the hookload values from the frictional models. This means that these three lines will be shown amongst all the black dots representing the true field data. See figure 3.2 below.

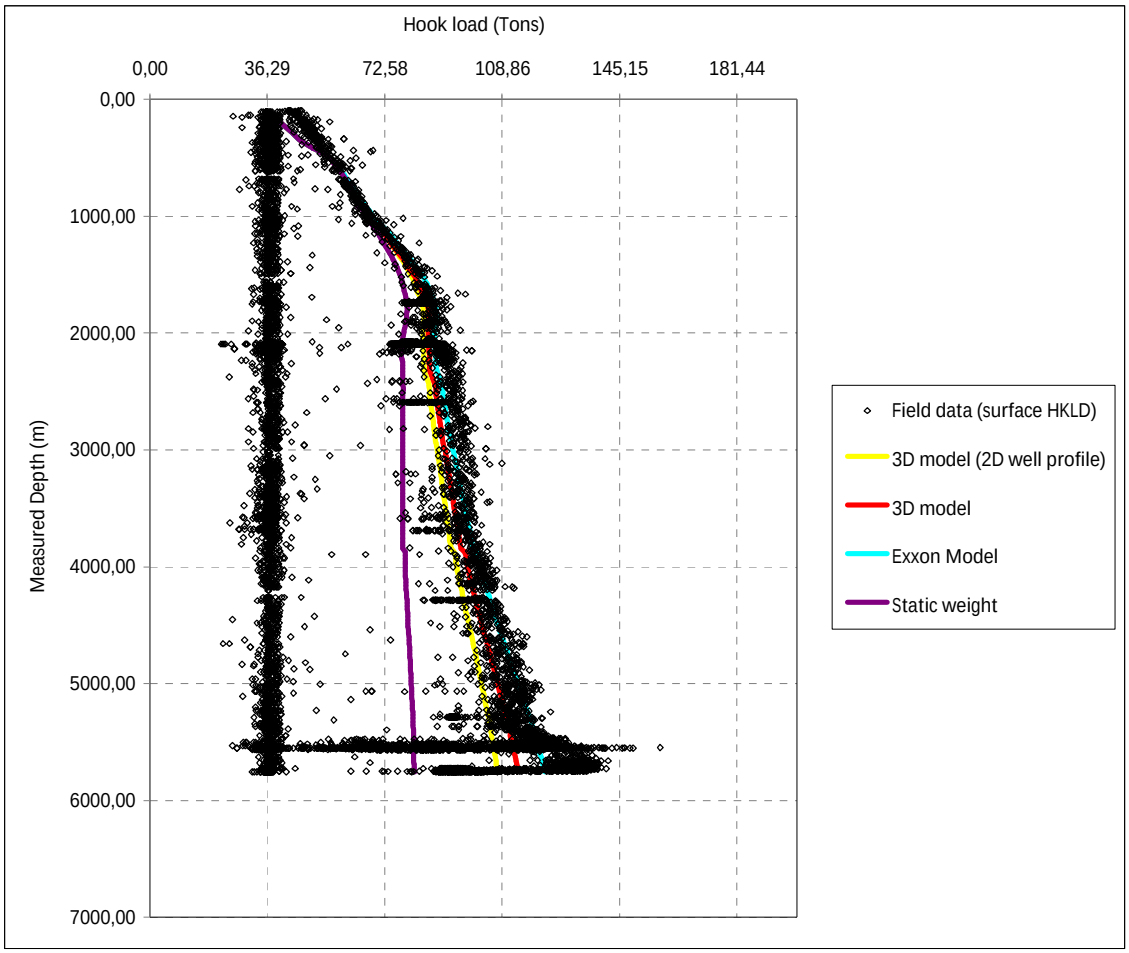

Figure 3.6: Example showing how calculated hookloads from the three different frictional models are plotted in the same diagram as field data hookloads and string static weight. Here: during a hoisting operation in well A with the friction factor, μ , = 0.2

This kind of a plot will be made for the operation of lowering the string and for hoisting of the string, depending on which kind of field data material one is dealing with, i.e. during which operation the material has been collected.

Common for the plots is that the plot will illustrate which calculated hookloads from the three frictional models that corresponds more to the true field data hookloads in the particular field case. When presented in a diagram, the difference between the frictional model hookload trend line (yellow, red and blue line above) and the line representing the static weight (purple line above), will be expressing the friction.

3.3.4.3 Differences between the two hookload plots

When lowering the string, one would below the kick-off point expect the three lines representing the calculated hookload values to be lying to the left of the static weight line (purple line above), since friction is reducing the hookload when the string is travelling down.

Likewise, when hoisting the string one would below the kick-off point expect the three lines representing calculated hookload values to be lying to the right of the line showing static string weight (purple line above). In this operation friction will be adding to the string weight.

3.3.4.4 Block weight/offset value

At the top section of the well, above the kick-off point, little friction should be present. Because of this fact, the colored and calculated hookload graphs should correspond more or less to the field data in this part of the diagram. See figure 3.4 below for illustration of this point.

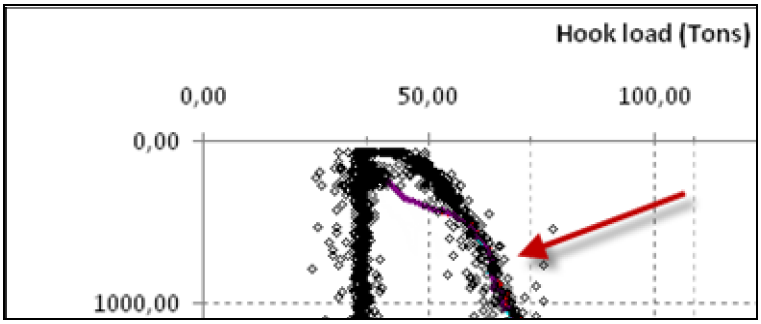

Figure 3.7: Material correspondence in top section of well. Here: during a lowering operation with the friction factor, m , = 0.2

The field data will include the block weight in its registrated hookload readings. The three calculation models on the other hand need to have this block weight added.

Therefore, it is necessary to contact the rig and get hold of this offset value. It will be incorporated into the document as previously mentioned (Chapter 3.2.2).

The degree of data material correspondence in this context can serve as a quick check on if some of the data has obvious lacks in any way. Also, it will be a check on if the provided block weight is a sensible one when used with the rest of the well material.

3.3.4.5 Discussion supportive plot I

Another plot to assist in discussing and understanding findings is one showing MD, mud flow rate and RPM vs. time. By interpreting such a plot, more can be said about which activities has taken place throughout the two well operations (RIH and tripping out). Because of lack of data, only MD vs. time was available for the B wells data set. See figure 3.8 for a plot example from well data set A.

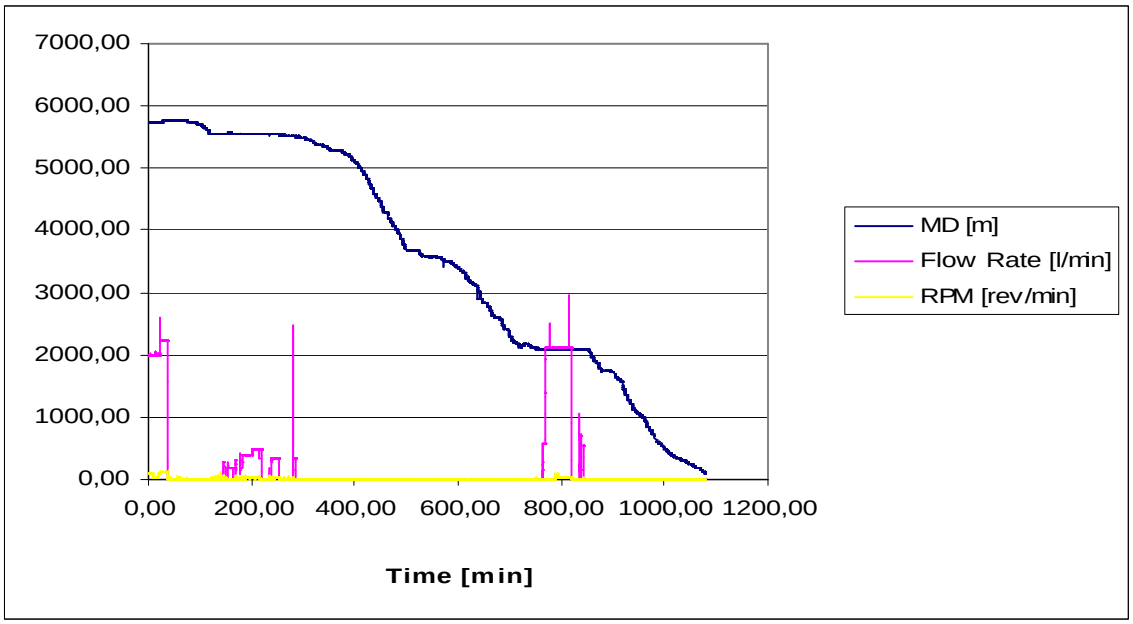

Figure 3.7: Plot showing MD, flow rate and RPM vs. time during a hoisting operation. The plot above is picked from well data set A.

3.3.4.5 Discussion supportive plot II

To get to see potential impacts from the use of an effective force, fluid side forces in a curved wellbore in kN was plotted against measured depth. In the same plot the pressure in bar of a static fluid in the wellbore was included. See figure 3.9 for a plot example from well data set B1.

When running a lower completion with annulus-tubing side hydraulically connected screens, and additionally filling the pipe every second stand, the annulus static fluid pressure is thought to be equal to the static fluid pressure inside the pipe ($p_o = p_i$).

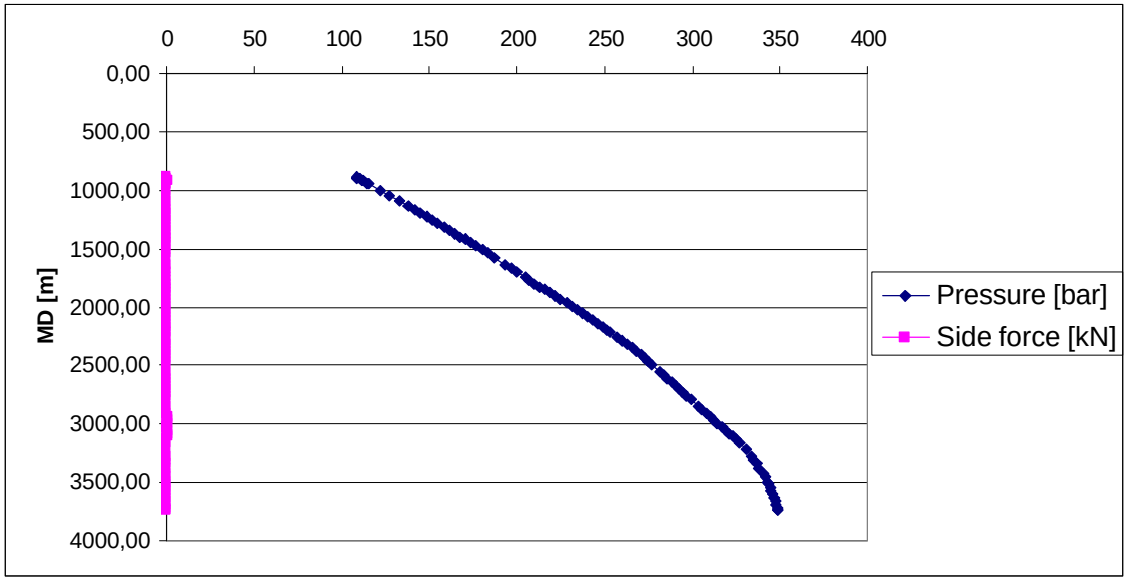

Figure 3.8: Plot showing fluid side force and pressure in a curved wellbore vs. measured depth. The plot above is picked from well data set B1.

4 Results

4.1 Introduction

This chapter is presenting the input data and the results from the experiments. The *results* to be presented are:

- Calculated and field measured hookloads when lowering the string (plot) with different friction factors for all wells
- Calculated and field measured hookloads when hoisting the string (plot) with different friction factors for well A

4.2 Uncertainty

4.2.1 Random uncertainty

Experimental errors that can be found if one repeats the experiments/measurements are called random errors. Since this thesis investigates the functionality of an excel spreadsheet, the results will be the same each time the data information is filled into the excel file. In this case, this thesis should not have random errors associated with it.[18]

4.2.2 Systematic uncertainty

Experimental errors that cannot be found if one repeats the experiments/measurements are called systemic errors. Possible systemic errors in this thesis can lie in the recorded data files received from offshore. There is no way to check if the readings slightly over- or underestimates values or if they are distorted in any other way. All offshore recordings need to be used the way they appear.[18]

The offshore block weight was conveyed over telephone and must be trusted to have that exact value, and thereby not having any systemic errors connected to it.[18]

4.3 Input data and results

4.3.1 Well data set A

The well data from well A is from an offshore North Sea well. A single run will be discussed. After a vertical top section, the well has a KOP at approximately 600 m TVD. From 600 m to 1600 m TVD the well builds a 90 degree inclination. The horizontal displacement after this is approximately 4000 meters, which makes this well a good candidate for a friction analysis. See figure 4.1 for a plot demonstrating this HD. Even though this run has a section being drilled close to TD, this analysis will only consider the RIH operation and the pulling-out of-hole. Figure 4.2 below is a plot showing the azimuth change and building of inclination vs. MD for this well.

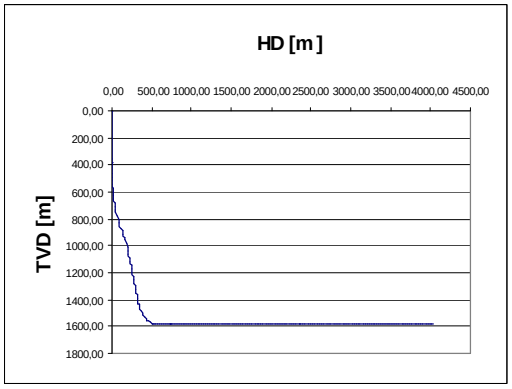

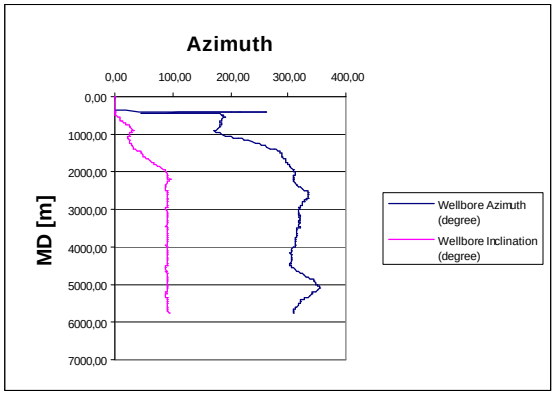

Figure 4.1 and 4.2: In figure 4.2 the horizontal displacement curve from well A treated in this experiment. It shows the Kick-off Point at approximately 600 meter TVD, and at 1600 meter TVD a long horizontal section is initiated. Figure 4.2 shows the azimuth and inclination vs. MD.

This well had a 5757 meter MD, was drilled with 1.12 s.g. and had a drill string consisting of 5 ½" 21 lbs/ft drill pipe in the top section and 5" 19.50 lbs/ft drill pipe in the lower section, with 5" 50.14 lbs/foot heavy weight drill pipe in the bottom section. The block weight was told to be 36 tons. See table 4.1 for more detailed info.

Table 4.1: Info on well A

MD [m]	TVD [m]	MW [s.g.]	Upper DP	Lower DP	Block weight
5757	1579	1,12	5 ½" 21 lbs/ft with 7 ¼" tool joint OD	5" 19.5 lbs/ft with 6 5/8" tool joint OD	36 tons

All the recorded offshore data from this well related to operations with a drill string.

4.3.2 Well data set B

The second well data set is from another source, an operator, and is from three different North Sea wells, but all from the same off shore field. They are relatively similar, have been drilled and completed the same year and followed the same running procedure. They will therefore here be treated in one chapter. As for well A, a single run will be considered. The wells all start vertically and have their KOP from right below the BOP at approximately 1000 m TVD. They then steadily build inclination throughout the wellbores until they reach the reservoir section. The reservoir for all wells is at right below 3000 m TVD, well inclination is then 81 degrees and the horizontal displacement is then approximately 1500 m for well B1 and B2, whereas B3 has a 650 m horizontal displacement. See figure 4.3, 4.5 and 4.7 for the TVD vs. horizontal displacement plots. This makes the wells horizontals, but not as horizontal as well A in terms of horizontal displacement and build angle. And since a completion string is run, after release from packer and screens downhole, the remaining string will be a regular drill string. Hence, only the operation lowering of completion string will be discussed here. Figures 4.4, 4.6 and 4.8 below show the azimuth change and building of inclination vs. MD for these wells.

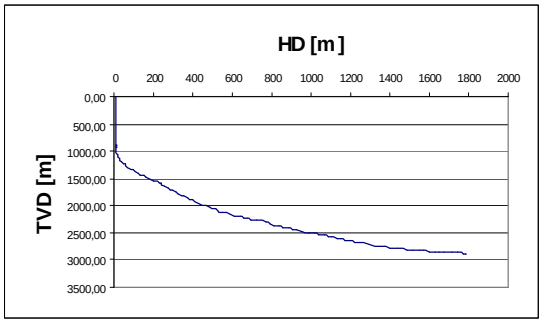

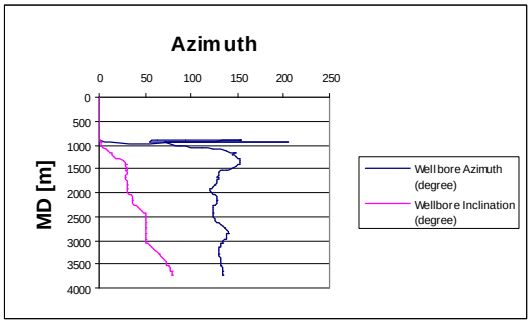

Figure 4.3 (left) and 4.4 (right): Horizontal displacement curve from the well B1 treated in this experiment to the left. It shows one each Kick-off Point at 1000 meter TVD and a long sail section ending with a close to 90 degrees section close to the bottom of the well. To the right the well azimuth and inclination plotted against MD.

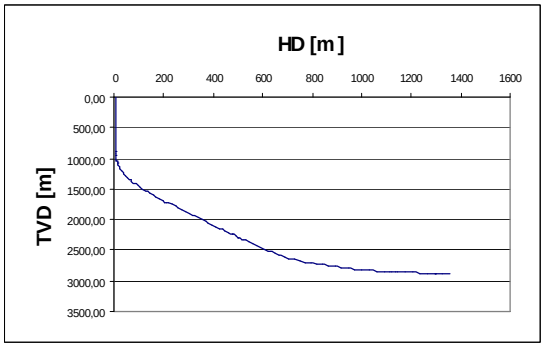

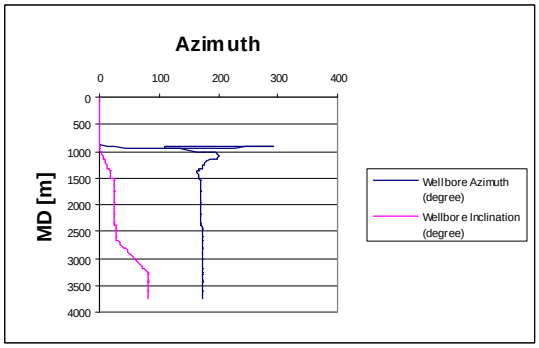

Figure 4.5 (left) and 4.6 (right): Horizontal displacement curve from the well B2 treated in this experiment to the left. It shows one each Kick-off Point at 1000 meter TVD and a long sail section ending with a close to 90 degrees section close to the bottom of the well. To the right the well azimuth and inclination plotted against MD.

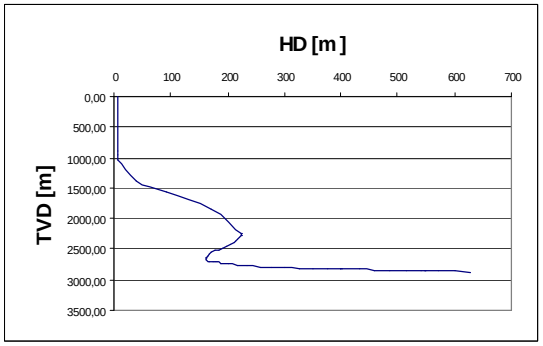

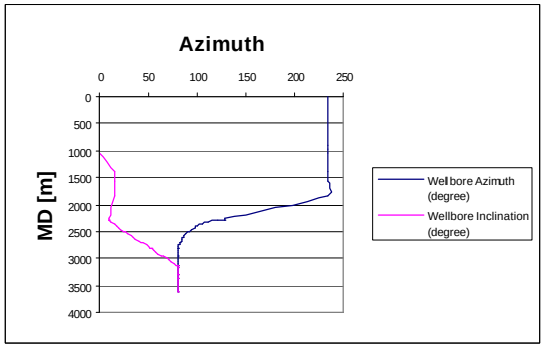

Figure 4.7 (left) and 4.8 (right): Horizontal displacement curve from the well B3 treated in this experiment. It shows two Kick-off Points, one at app 1000 meter TVD and the other one at app 2700 meter. After this a long sail section ending with a long, close to 90 degrees, section close to the bottom of the well. To the right the well azimuth and inclination plotted against MD.

The BOP was situated on the seafloor at 880 meter for all three wells, and their first kick-off point was below this point. The wells had measured depths of 3858 meter (B1), 3516 meter (B2) and 3390 meter (B3). The lower completions were all run in 1,24 s.g. brine and had a relatively differentiated completion string, but more or less the same string for all three wells. The string was differentiated because of different concerns like one wanting to use a yield strong pipe in the top section, another drill pipe through the BOP and the 9 5/8" casing, the stiff HWDP to avoid buckling, in addition to the different completion components of the string. See table 4.3 below for details on such a string. The block weight was informed from the rig to be 39 tons. See table 4.2 for a summary of the well info.

Table 4.2: Info on wells B1, B2 and B3

MD [m]	TVD [m]	MW [s.g.]	Upper DP	Lower DP	Block weight
3858 3516 3390	2870 2892 2872	1,24	See table 4.3	See table 4.3	39 tons

Table 4.3: The B1 completion string

Tool type	Max OD [in.]	Actual weight [lbs/ft]	Length [m]
5" V150 DP	6 5/8	33,8	870
5 ½" FH DSTJ DP	7,00	25,24	1200
5" DP	6 5/8	22,61	400
5" HWDP	6	49,7	350
5" DP	6 5/8	22,61	806
5" HWDP	6 ½	49,7	56
GP Assy w/ innerstring	8,313	65,0	16
7" 32# Blank w/ innerstring	7	41,5	45
5 ½" 17# screen w/ innerstring	6,05	28,0	150

All the recorded offshore data from this well related to operations with a completion string.

4.3.3 Plots and results

The results from well A are presented as plots showing the hoisting and lowering of one particular run of the drill string into the well. This can be considered to be some sort of a

baseline experiment, since similar case studies have been thoroughly analyzed by Mirhaj, Kaarstad and Aadnoy in 2010. After several iterations a friction factor was determined, and the latest version of a calibrated spreadsheet and its experimental results were ready and complete for this well.

The exact same spreadsheet was then used for the running of a lower completion string into the B wells. However, for the B wells plots are only shown for the running (lowering) of the lower completion string. Since the lower completion (packer, screens and more) is left downhole, the hoisting operation will only be of a conventional and remaining shorter drill pipe string and has not been considered here.

All the plots are shown with a friction factor that has been chosen through the trial and error method. Plots with a friction factor right below and right above the plots with the best fit factor, are attached in the appendix. Additionally, for the running of the three completion strings, the friction factor is empirically known to be just above 0.3.

4.3.3.1 m = 0.25 during lowering of drill string into well A

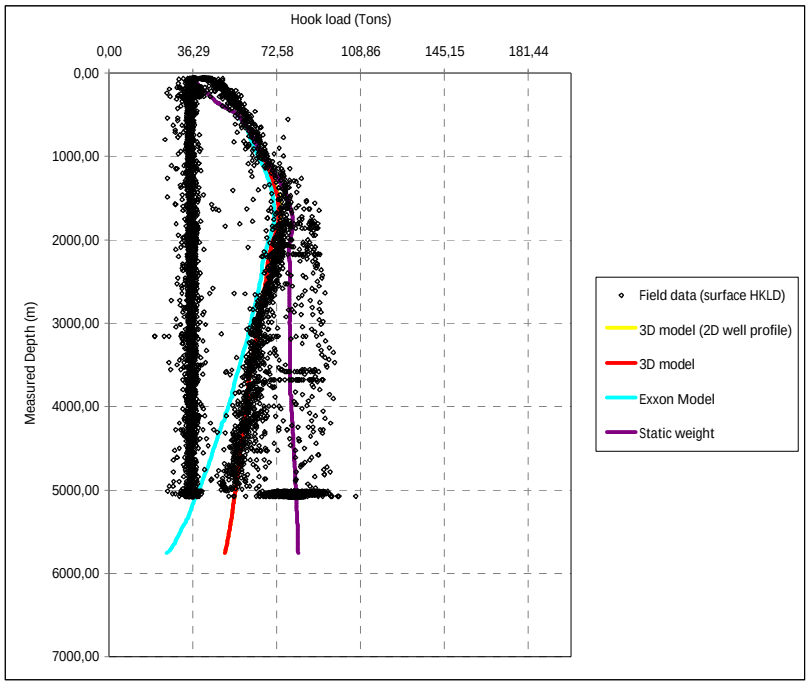

Figure 4.9: Lowering of drill string into well A when m = 0.25

4.3.3.2 m = 0.25 during hoisting of drill string from well A

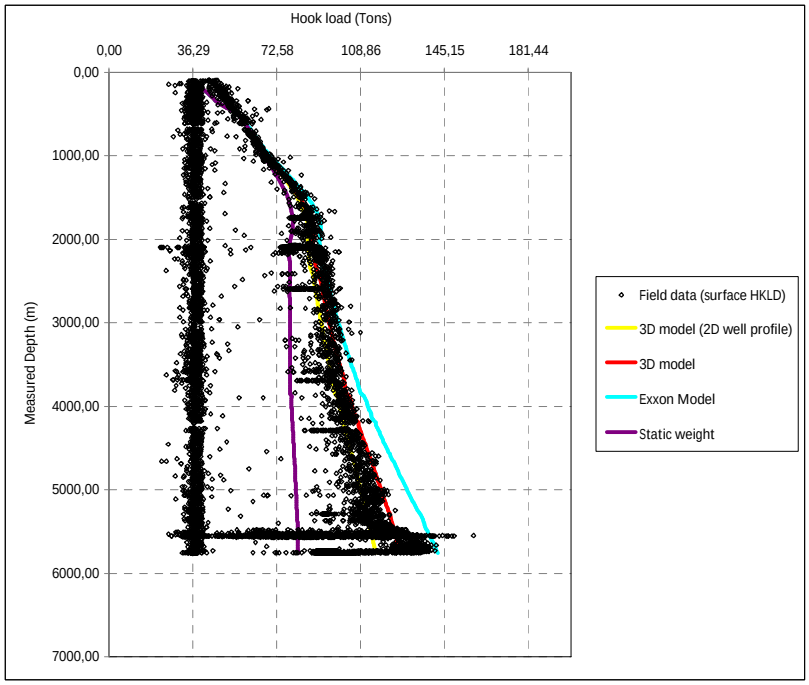

Figure 4.10: Hoisting of drill string from well A when m = 0.25

4.3.3.3 m = 0.3 during lowering of completion string into well B1

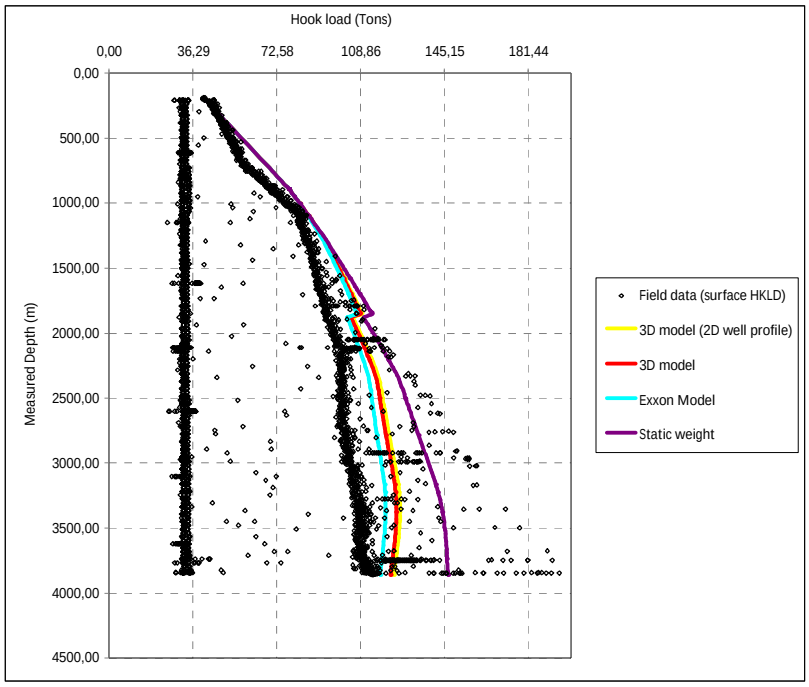

Figure 4.11: Lowering of completion string into well B1 when m = 0.3

4.3.3.4 m = 0.3 during lowering of completion string into well B2

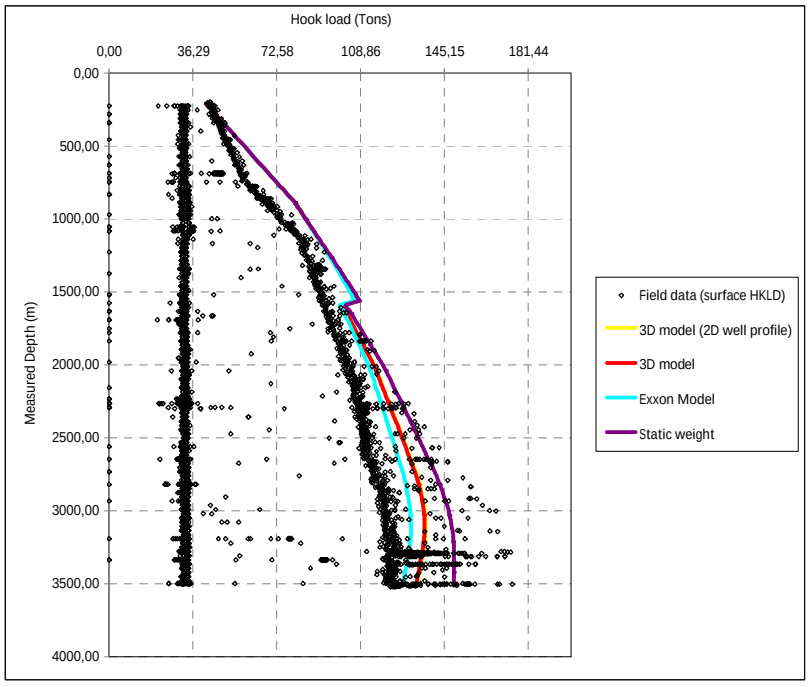

Figure 4.12: Lowering of completion string into well B2 when m = 0.3

4.3.3.5 μ = 0.3 during lowering of completion string into well B3

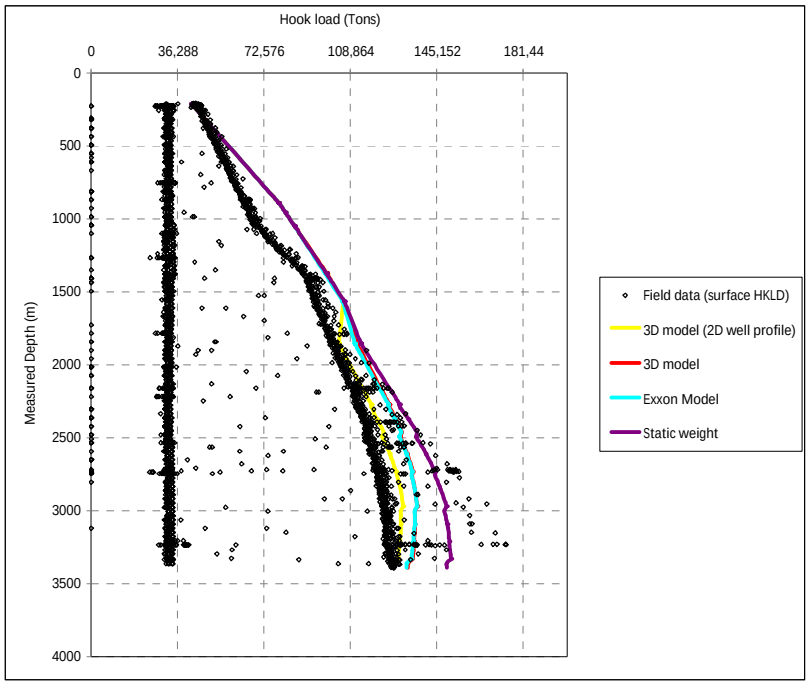

Figure 4.13: Lowering of completion string into well B3 when μ = 0.3

4.3.4 Other plots

Below are plots showing measured depth, flow rate and RPM vs. time for well A, and measured depth vs. time for the B wells. The very last plot illustrates the fluid side force and pressure in a curved wellbore vs. measured depth and is from well data set B1 only.

4.3.4.1 Hoisting operation well A

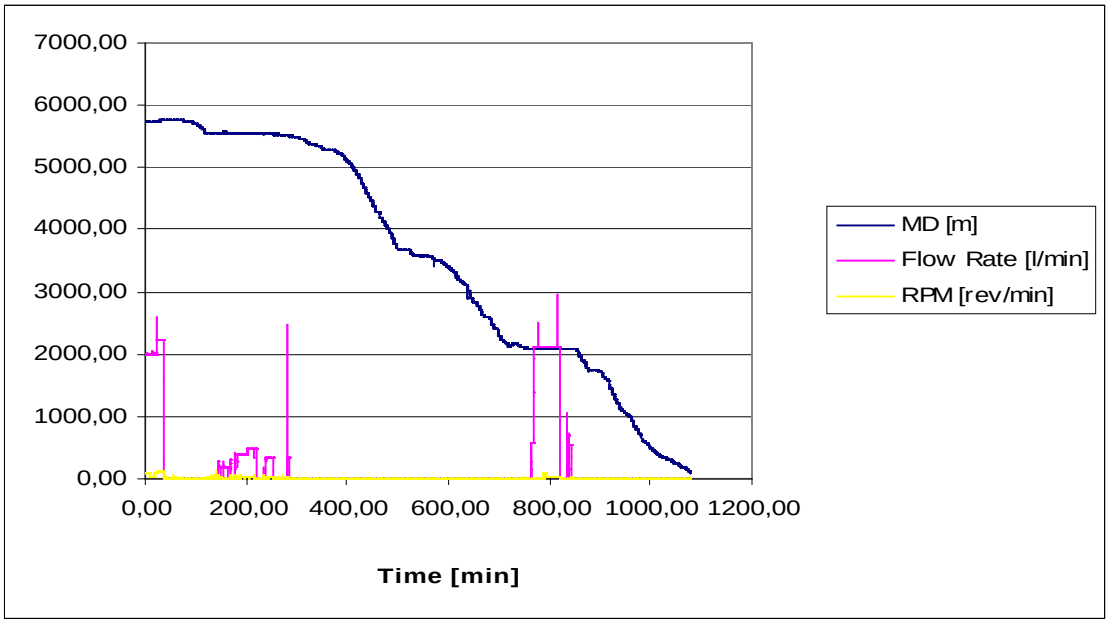

Figure 4.14: MD, flow rate and RPM vs. time during the hoisting operation in well A

4.3.4.2 Lowering operation well A

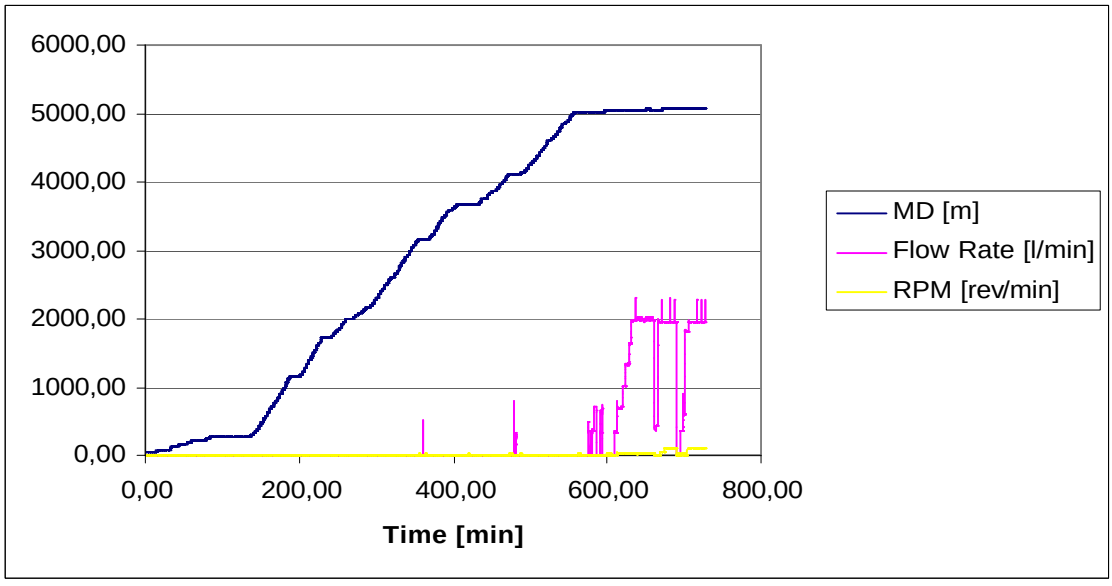

Figure 4.15: MD, flow rate and RPM vs. time during the lowering operation in well A

4.3.4.3 Lowering operation well B1

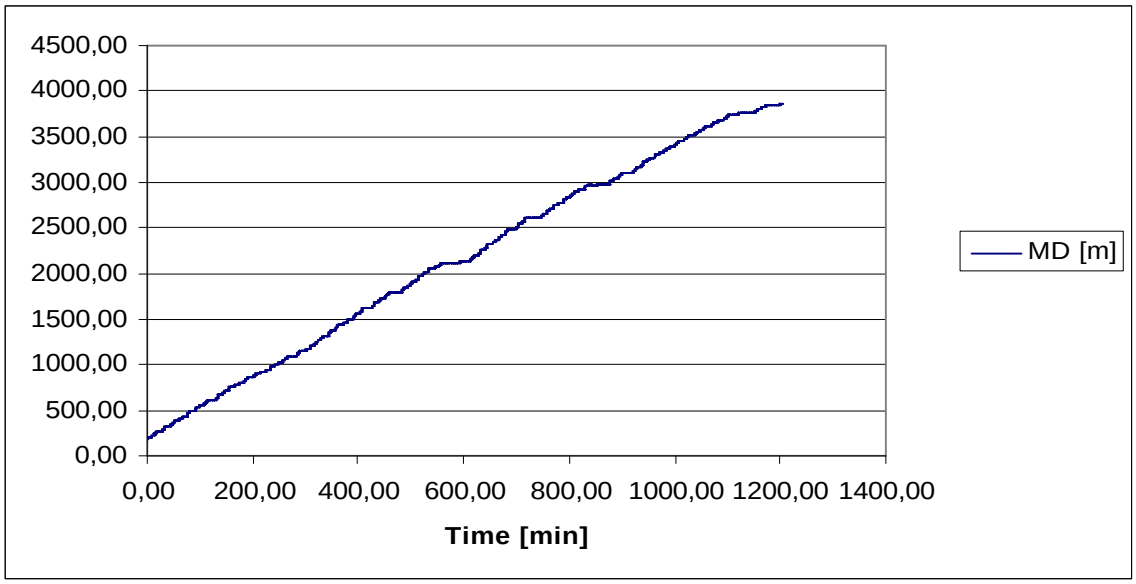

Figure 4.16: MD vs. time during the lowering operation in well B1

4.3.4.4 Lowering operation well B2

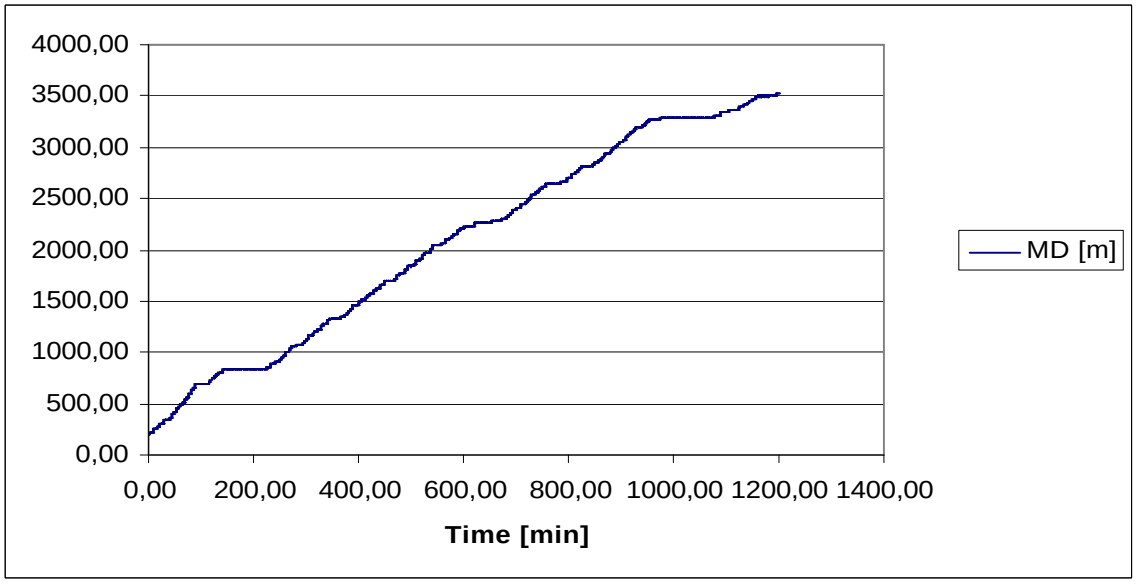

Figure 4.17: MD vs. time during the lowering operation in well B2

4.3.4.5 Lowering operation well B3

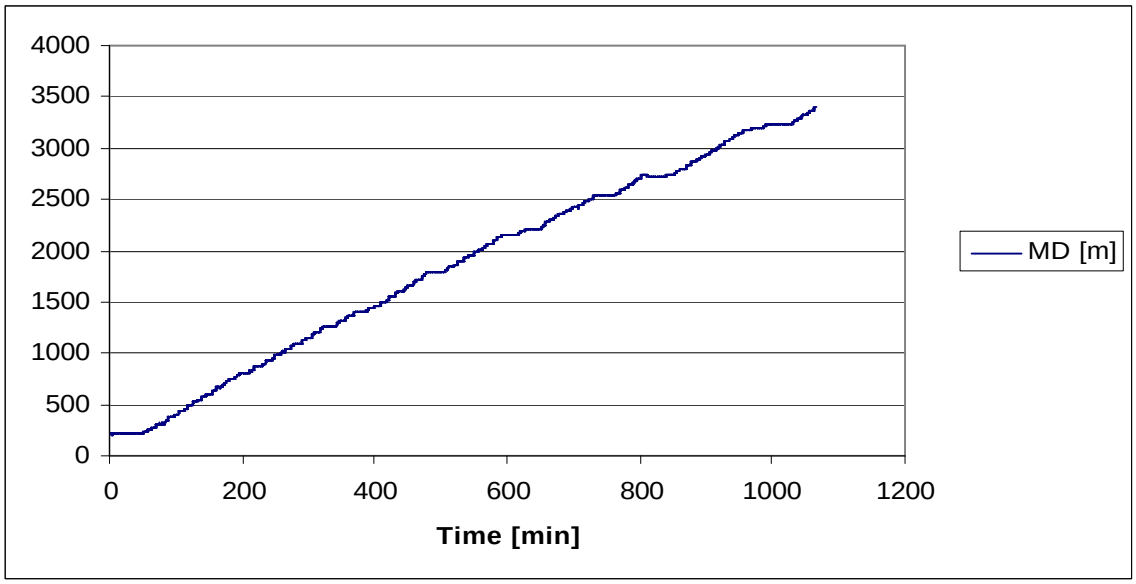

Figure 4.18: MD vs. time during the lowering operation in well B3

4.3.4.5 Well B1

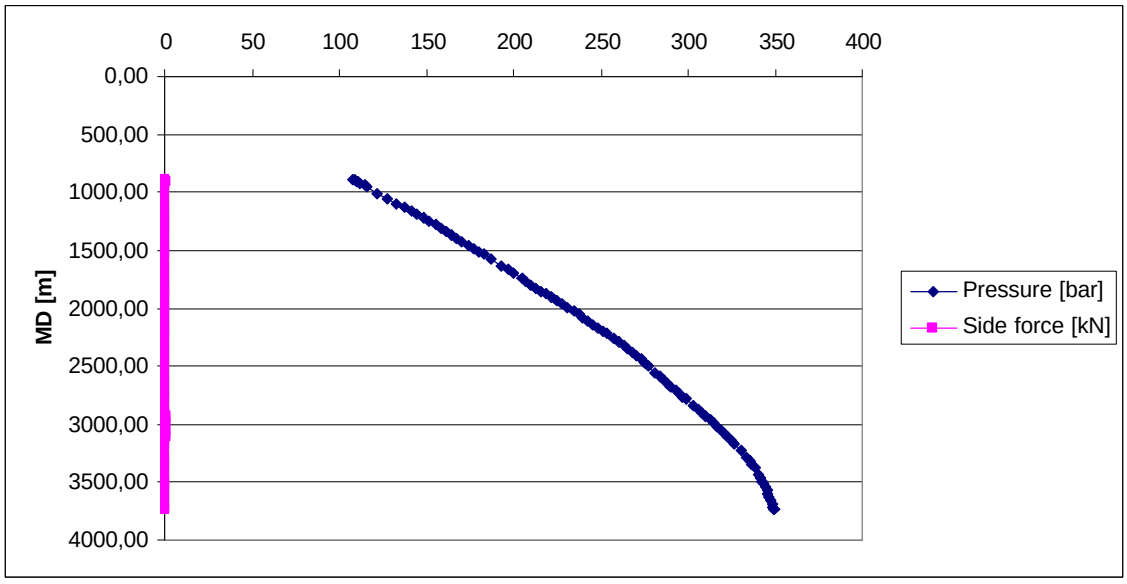

Figure 4.19: Fluid side force and pressure vs. measured depth in well B1

5 Discussion

5.1 Well data set A – tripping out with a drill string

The well A data material has been trialed with different friction factors to see how different the values would impact on the degree of match between predicted and actual hookload values. One friction factor was chosen for the whole of the well interval, instead of differentiating between an open hole section and a cased hole section friction factor.

The friction factor that showed the best match with the hookload data when used in the prediction models was 0.25. The limit value friction factors right above and right below 0.25 were also utilized to create plots and are found in the appendix chapter A-1 through A-4. These friction factors were 0.2 and 0.3 respectively.

As can be seen from figure 4.10 in the results chapter, there is a relatively good correspondence between the 3D model predicted hookload data and the actual hookload data in the particular case of hoisting the drill string out from well A in this experiment. From bottom and upwards, some comments can still be made.

At bottom, the string took some over-pulls when trying to move out from the recently drilled section. This can be seen on the very bottom in figure 4.10. To get loose and keep POOH, circulation with lubricants at 400 lpm was commenced. This can again be seen from figure 4.14 (the purple line down to the left in the plot, right to the right of the part of the flow rate showing the displacing of the open hole mud at 2000 lpm).

In addition to the fact that the string had some over-pulls in this very bottom section of the well, this is one of the sections that experience the greatest azimuth changes, see figure 4.2. Great azimuth changes in the horizontal section can be associated with a reduced validity of the soft string friction prediction models, and hence under-prediction of the friction (and hookloads).

The excel spreadsheet used in these experiments does however try to capture these side-bend effects in the horizontal section. A tension limit value has been introduced to the thesis spreadsheet, even though not being trialed here, this tension limit has been set to a fixed value in all the experiments. After this, the excessive hookloads in the bottom of the wellbore probably is owing to the over-pulls rather than the azimuth changes in the horizontal section.

The other azimuth change in the horizontal section occurs at +/- 2500 meters. Despite of the introduction of the tension limit value to the spreadsheet, there are tendency to some increased hookloads in this area as well.

Above the section with slightly higher hookloads (2600-2900 m), correspondence between prediction models and actual hookloads again arise. Worth noticing may here again be figure 4.14. The figure shows a riser and casing displacing procedure taking place at 2100 m MD. The well is displaced to 1.25 s.g. sized salt mud. This does not seem to impact on the hookloads. On the contrary, better correspondence between the curves seems to be the case in this area. Maybe this can be due to a buoyancy effect.

Getting close to the top section, there will be lesser hookload and inclination (close to the vertical section). After having pulled the string through the inclination build section of the well, closer correspondence between the curves is expected.

At the very top, in the vertical section, the static weight falls beneath the plotted hookload dots. This will relate to the survey material attached in the Appendix Table A-1, where the well data set A survey is found. The survey lacks information on the uppermost 361 meters.

5.2 Well data set A – tripping in with a drill string

Much the same picture is seen in well data set A when tripping in, see figure 4.9. The same top section discrepancy due to the survey lacks is found, and a relatively good match between the 3D model and the actual hookloads is found throughout the wellbore.

The pipe filling procedure is in this case not to fill the pipe every 1000 meters. Accordingly, the hookloads do not increase every 1000 meters. This is then an expected finding. Also figure 4.15 shows no breaks in time during reaching MD due to filling of the pipe.

Figure 4.15 does however show when preparations for drilling start are commenced, after approximately 600 minutes. At this point in time establishing of circulation begins.

5.3 Well data set B – tripping in with a completion string

5.3.1 General findings

Whereas the hookloads decrease when the drill string enters the horizontal section at approximately 1600 meter TVD in the case of the well data set A figure 4.9, this is not the case in the plots showing the lowering of a completion string into wells B1, B2 and B3 (figures 4.11 through 4.13). The hookloads do not decrease as steeply during the tripping in with the completion strings, in fact the hookloads keep increasing all the way down to TD. The B wells have smaller inclination and a shorter horizontal section. Hence, the hookload reduction due to friction should be more moderate in the B wells than in the A well.

The pipe is in this operation according to the daily operations report filled with mud every second stand, hence the pattern seen when pipe filling takes place every 1000 meter is not present. This can further be supported by plots 4.16 through 4.18, as no breaks are seen – but rather a steady increase of MD vs. time.

Figures 4.11 through 4.13 show that on occasion during lowering, the completion strings has taken weight.

5.3.2 Degree of match between 3D model and hookload data

It is striking nevertheless that there are relatively large discrepancies in all plots between all the prediction models and the hookload data. The torque and drag models over-predict the hookloads in all three wells. The only place, where there is a match between the prediction models and the hookload data is in well B1, at 1000 meter where there also is an excessive azimuth change.

The friction factor that has been used in these simulations is 0.3. This factor has been found empirically from the deep clean-up run prior to the running of the lower completion, and should therefore be a reasonable value. As can be seen in the Appendix Figures A-5 through A-10, choosing a friction factor of 0.2 or 0.4 would not really impact much on the results either.

The excel spreadsheet does have an un-differentiated drill string data info box. The completion string for these three particular wells undergoes component dimension change eight times throughout the wellbore, whereas the spreadsheet drill string data editor only allows for two such changes. Because of this, some discrepancy should be anticipated. There is however a consistent over-prediction of the hookloads in all wells all throughout the wellbore. An undifferentiated drill string data editor cannot suggest an explanation to all of this.

5.3.3 Effect from use of the effective pressure force in a curved wellbore

An attempt has been done to investigate potential impacts from the use of the effective downhole pressure force, which includes the effects of surrounding fluid on the pipe in a curved wellbore. One figure only demonstrates an examination of these effects. Figure 4.19 illustrates the size of fluid side forces when used on the well data set B1. As it is relatively clearly seen from the plot, these forces are of no significant magnitude in this particular case.

6 Conclusion

This thesis has been a continuation of work done by Mirhaj, Kårstad and Aadnøy (paper published in 2010) and Mirhaj, Fazaelizadeh, Kårstad and Aadnoy (paper published in 2010) on the functionality of a 3-dimensional friction model. More material has now been analyzed by use of an excel spreadsheet from 2009, taking into account forces acting in side bends in the horizontal section of the wellbore.

The 3-dimensional friction model excel spreadsheet was applied on the operation lowering of a completion string, in addition to on the operations hoisting and lowering of a drill string. Whereas there was a relatively good correspondence between all prediction models and the hookload data in the case of hoisting and lowering of a drill string, this was not the case for the lowering of a completion string. The completion string has somewhat different qualities than a conventional drill string, and an in this case differentiated completion string could not fully be taken into account by the experimental excel spreadsheet, as the spreadsheet appears today.

An attempt to examine if the effect of surrounding fluids on the pipe in a curved wellbore could suggest an explanation to the reduced correspondence in the case of the running of a completion string was done. No such connection was found.

References

1 Mirhaj, S.A., Kårstad, E., Aadnoy, B.S., “Minimizing Friction in Shallow Horizontal Wells”, SPE 135812, IADC/SPE Asia Pacific Drilling Technology Conference and Exhibition, Ho Chi Minh City, Vietnam, November 2010.

2 Mirhaj, S.A., Fazaelizadeh, M., Kårstad, E., Aadnoy, B.S., “New Aspects of Torque-and-Drag Modeling in Extended-Reach Wells”, SPE 135719, SPE Annual Technical Conference and Exhibition, Florence, Italy, September 2010.

3 Johancsik, C.A., Friesen, D.B., Dawson, R., “Torque and Drag in Directional Wells – Prediction and Measurement”, *Journal of Petroleum Technology*, June 1984.

4 Sheppard, M.C., Wick, C., Burgess, T., “Designing Well Paths To Reduce Drag and Torque”, *SPE Drilling Engineering*, December 1987.

5 Lesage, M., Falconer, I.G., Wick, C.J., “Evaluating Drilling Practice in Deviated Wells With Torque and weight Data”, *SPE Drilling Engineering*, September 1988.

6 Brett, J.F., Beckett, A.D., Holt, C.A., Smith, D.L., “Uses and Limitations of Drillstring Tension and Torque Models for Monitoring Hole Conditions”, *SPE Drilling Engineering*, September 1989.

7 Aarrestad, T.V., Blikra, H., “Torque and Drag – Two Factors in Extended-Reach Drilling”, *Journal of Petroleum Technology*, September 1994.

8 Payne, M.L., Abbassian, F., “Advanced Torque-and-Drag Considerations in Extended-Reach Wells”, *SPE Drilling &* Completion, March 1997.

9 Opeyemi, A.A., Pham, S.V., “A Robust Torque and Drag Analysis for Well Planning and Drillstring Design”, SPE/IADC 39321, presented at SPE/IADC Drilling Conference, Dallas, Texas, March 1998.

10 Aadnøy, B.S., Andersen, K., “Friction Analysis for Long-Reach Wells”, SPE/IADC 39391, presented at SPE/IADC Drilling Conference, Dallas, Texas, March 1998.

11 Reiber, F., Vos, B.E., Eide, S.E., “On-Line Torque & Drag: A Real-Time Drilling Performance Optimization Tool”, SPE/IADC 52836 presented at the SPE/IADC Drilling Conference, Amsterdam, Netherlands, March 1999.

12 Rae, G., Lesso jr., W.G., Sapijanskas, M., “Understanding Torque and Drag: Best Practices and Lessons Learnt from the Captain Field’s Extended Reach Wells”, SPE/IADC 91854 presented at the SPE/IADC Drilling Conference, Amsterdam, Netherlands, February 2005.

13 Aadnøy, B.S., Fabiri, V.T., Djuurhus, J., “Construction of Ultralong Wells Using a Catenary Well Profile”, SPE/IADC 98890 presented at the SPE/IADC Drilling Conference, Miami, February 2006.

14 Aadnøy, B.S., Djuurhus, J., “Theory and Application of a New Generalized Model for Torque and Drag”, SPE/IADC 114684 presented at the IADC/SPE Asia Pacific Drilling Technology Conference and Exhibition, Jakarta, Indonesia, August 2008.

15 Mitchell, R.F., Samuel, R., “How Good Is the Torque/Drag Model?” *SPE Drilling & Completion*, March 2009.

16 Inglis, T.A., “Directional Drilling”, Graham & Trotman, 1987.

17 Aadnoy, B.S., “Mechanics of Drilling”, Shaker Verlag, 2006.

18 Taylor, J.R., “An Introduction to Error Analysis”, University of Colorado, 1997.

19 Aadnoy, B.S., Fazaelizadeh, M., Hareland, G., “A 3-Dimensional Analytical Model for Wellbore Friction”, *Journal of Canadian Petroleum Technology*, 2010.

20 Fazaelizadeh, M., Hareland, G., Aadnoy, B.S., “Application of the New 3-D Analytical Model for Directional Wellbore Friction”, Journal of Modern Applied Science, Vol. 4, No. 2, 2010.

21 Mitchell, R.F., “Fluid Momentum Balance Defines the Effective Force”, SPE/IADC 119954 presented at the SPE/IADC Drilling Conference and Exhibition, Amsterdam, The Netherlands, March 2009.

Appendix

Figure A-1: Lowering of drill string into well A when m = 0.2

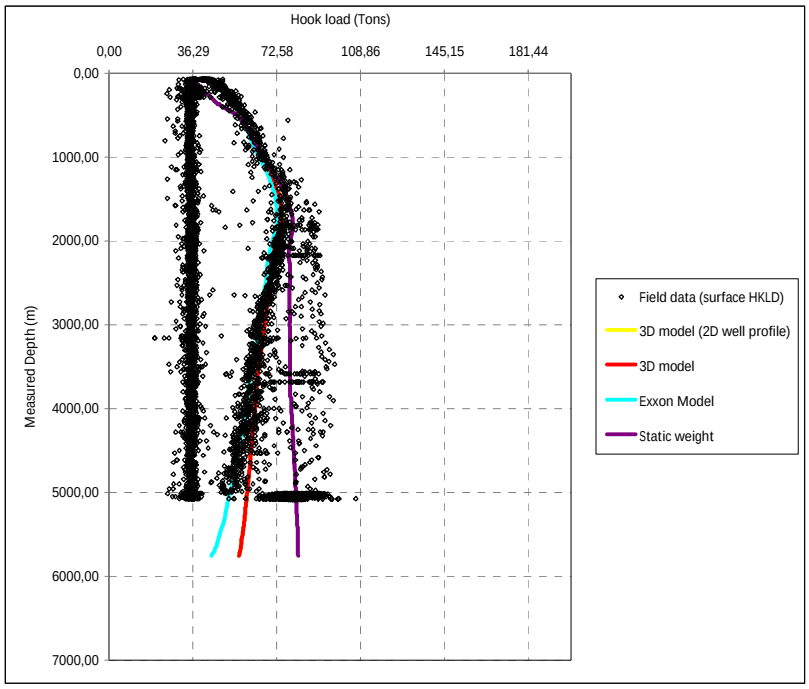

Figure A-2: Hoisting of drill string from well A when m = 0.2

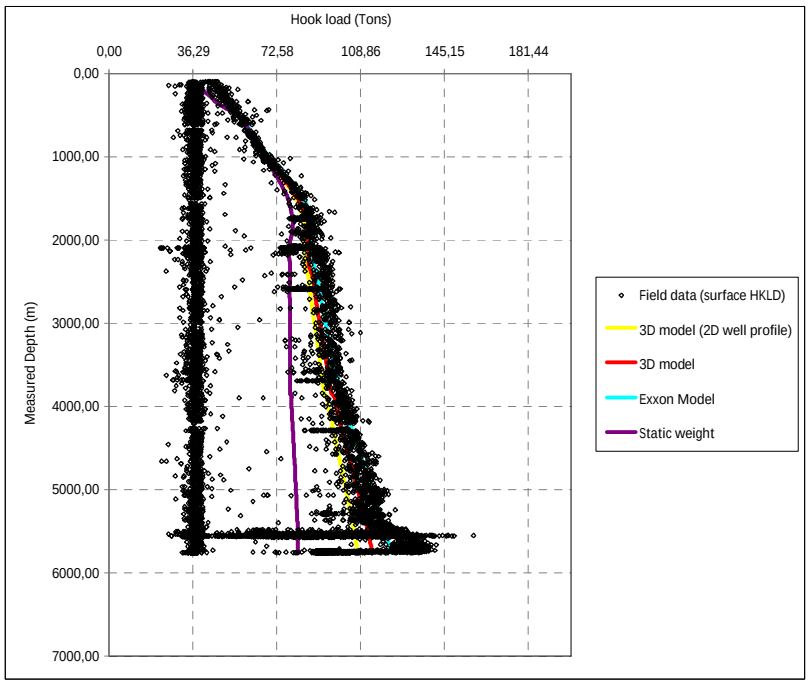

Figure A-3: Lowering of drill string into well A when $m = 0.3$

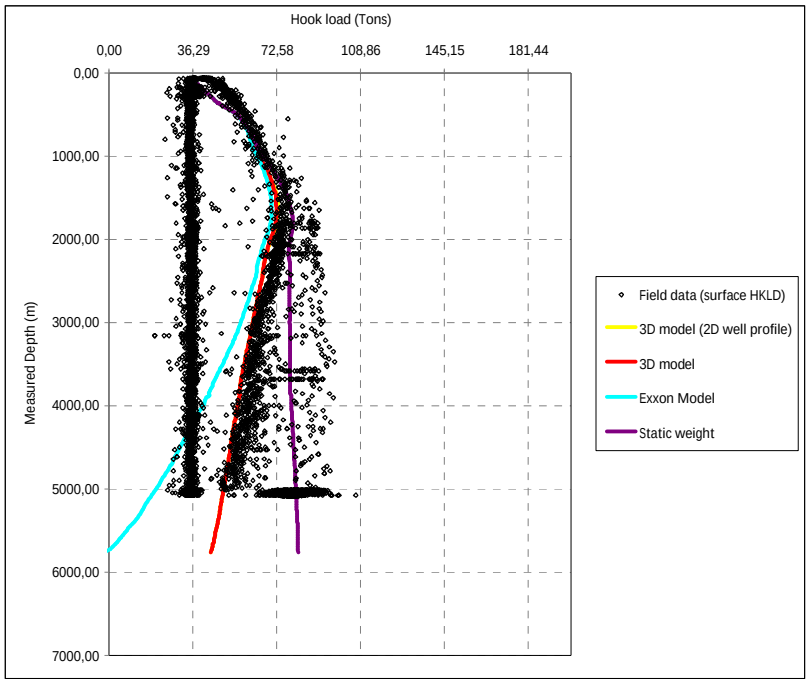

Figure A-4: Hoisting of drill string from well A when $m = 0.3$

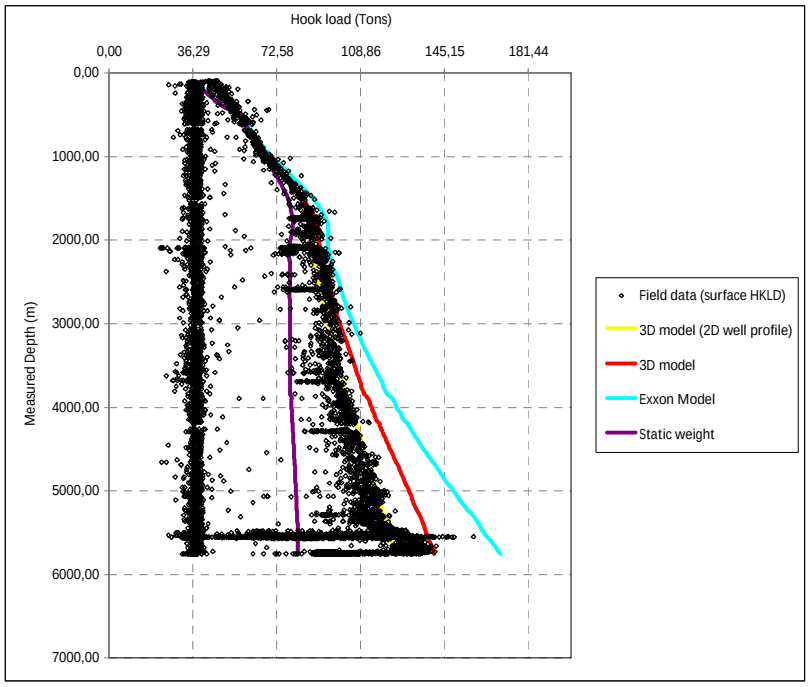

Figure A-5: Lowering of completion string into well B1 when m = 0.2

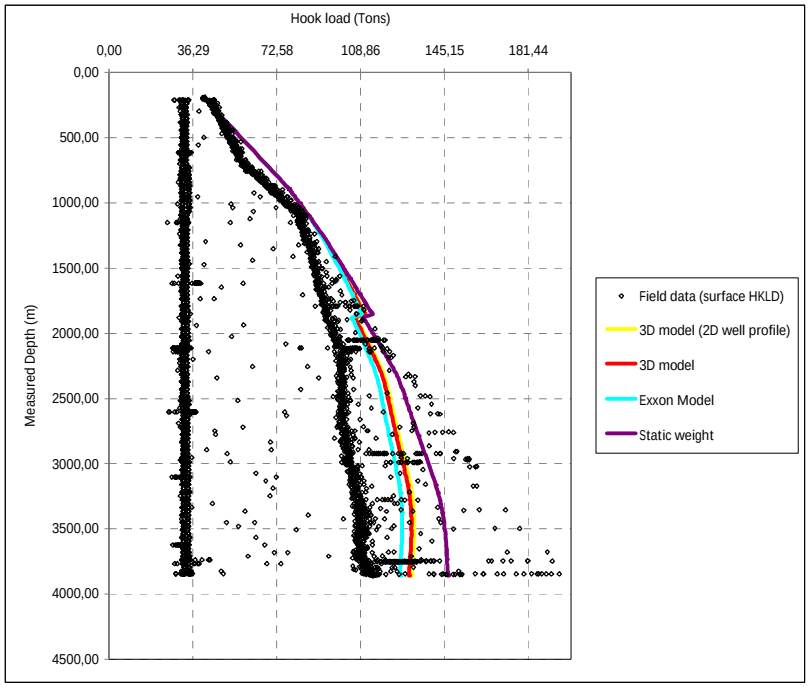

Figure A-6: Lowering of completion string from well B1 when m = 0.4

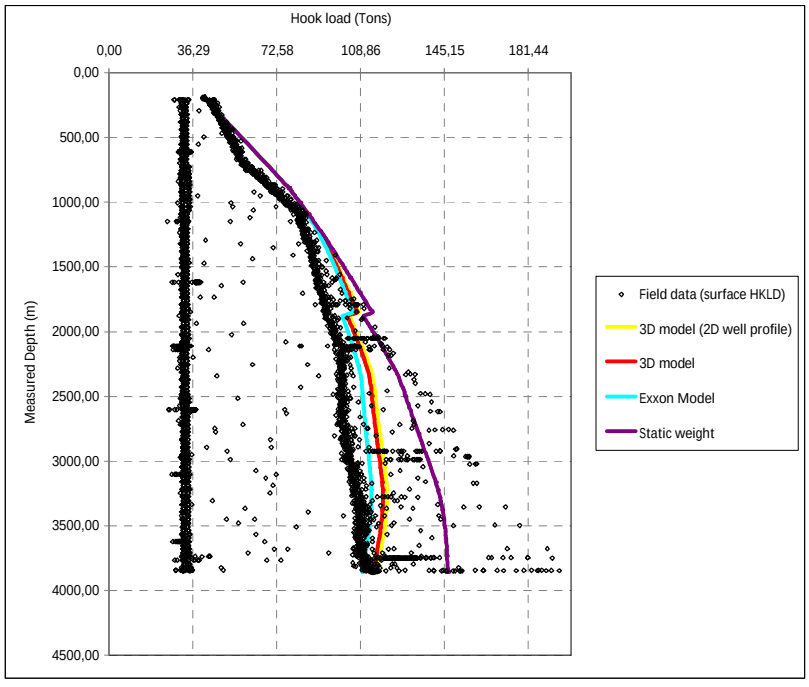

Figure A-7: Lowering of completion string into well B2 when $m = 0.2$

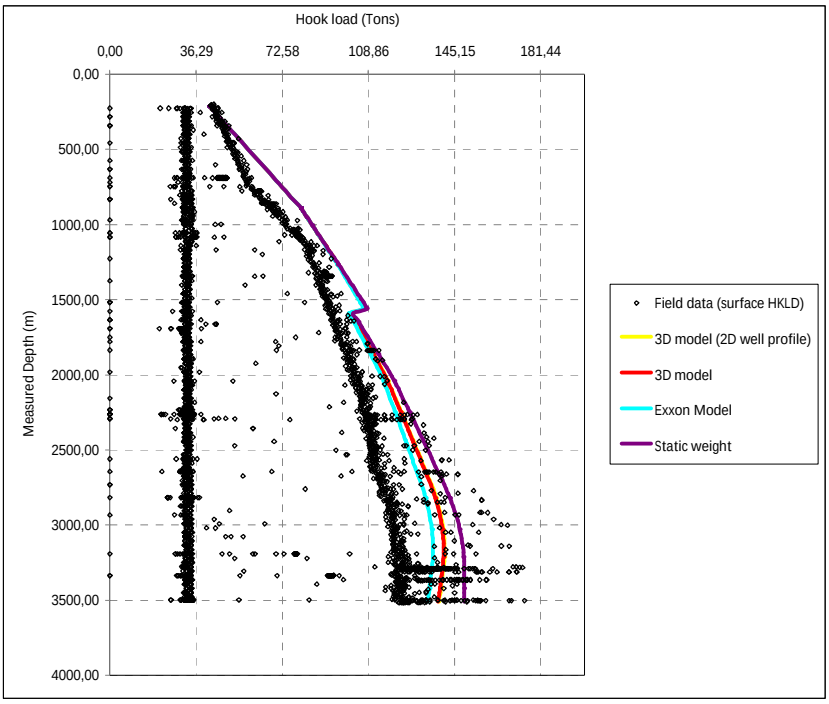

Figure A-8: Lowering of completion string into well B2 when $m = 0.4$

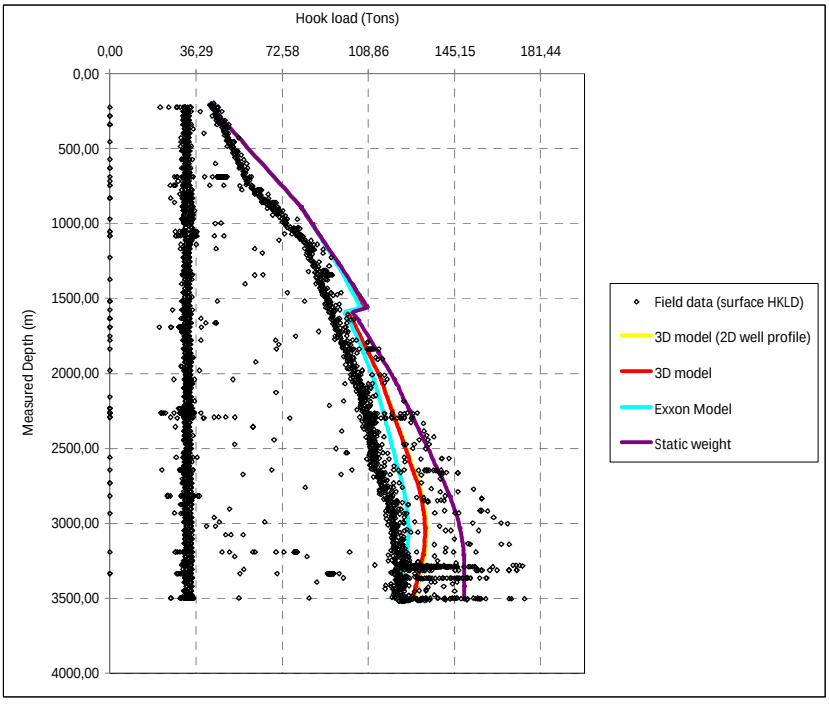

Figure A-9: Lowering of completion string into well B3 when $m = 0.2$

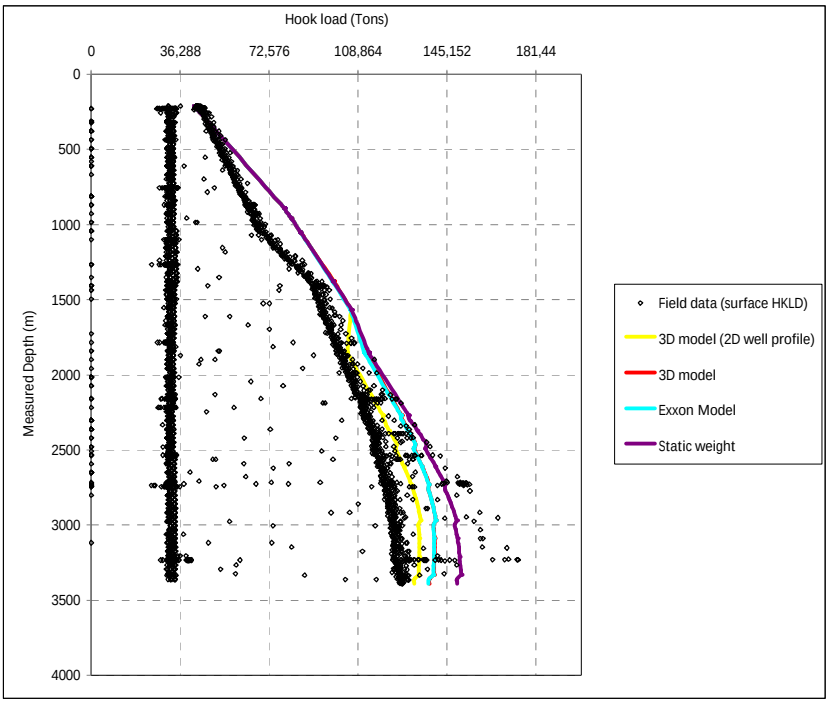

Figure A-10: Lowering of completion string into well B3 when $m = 0.4$

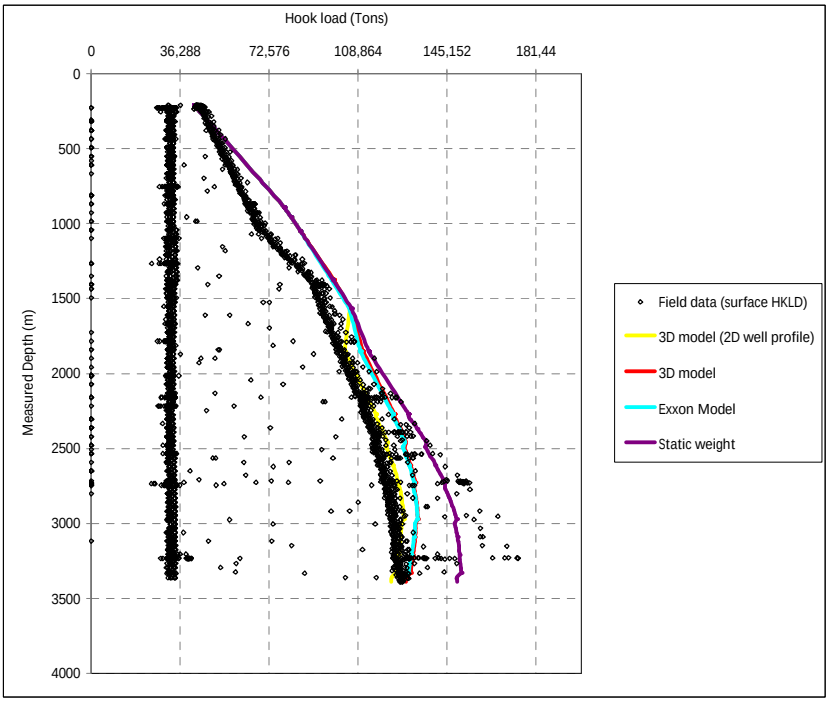

Table A-1: Well A survey

MD [m]	Inclination [°]	Azimuth [°]	TVD [m]	Vert Sect [m]	North [m]	East [m]	DLS [°/30m]
0,00	0,00	0,00	0,00	0,00	-1,90	-4,80	0,00
3,00	0,00	0,00	3,00	0,00	-1,90	-4,80	0,00
361,20	0,00	0,00	361,20	0,00	-1,90	-4,80	0,00
378,00	0,55	213,80	378,00	-0,01	-1,97	-4,85	0,98
386,00	0,40	217,40	386,00	-0,02	-2,02	-4,89	0,57
396,00	0,28	263,80	396,00	-0,01	-2,05	-4,93	0,87
405,00	0,51	259,70	405,00	0,02	-2,06	-4,99	0,77
417,00	0,62	201,30	417,00	0,03	-2,13	-5,07	1,40
435,00	0,15	44,60	435,00	-0,01	-2,21	-5,09	1,27
461,00	0,73	171,90	461,00	-0,14	-2,35	-5,04	0,96
485,00	1,58	187,80	484,99	-0,46	-2,82	-5,06	1,13
514,00	3,06	183,80	513,97	-1,20	-3,99	-5,17	1,54
544,00	5,66	189,50	543,88	-2,56	-6,25	-5,47	2,63
572,00	8,19	190,50	571,67	-4,45	-9,57	-6,06	2,71
601,00	9,68	184,90	600,32	-7,15	-14,04	-6,64	1,78
630,00	11,49	185,70	628,83	-10,49	-19,34	-7,14	1,88
660,00	13,43	182,00	658,12	-14,69	-25,79	-7,56	2,10
689,00	15,95	182,20	686,17	-19,63	-33,14	-7,83	2,61
717,00	19,01	183,90	712,87	-25,15	-41,54	-8,28	3,32
742,00	19,78	185,72	736,45	-30,42	-49,81	-8,98	1,17
750,00	21,25	182,35	743,95	-32,23	-52,61	-9,18	7,08
793,00	24,47	182,50	783,56	-43,37	-69,29	-9,89	2,25
822,70	26,65	181,00	810,36	-52,02	-82,10	-10,27	2,30
851,40	28,48	177,29	835,80	-61,43	-95,37	-10,06	2,62
890,60	31,83	172,15	869,69	-76,42	-114,96	-8,20	3,23
909,30	33,09	173,27	885,47	-84,28	-124,91	-6,93	2,24
939,90	30,60	177,10	911,47	-96,48	-140,99	-5,56	3,14
968,00	28,87	180,68	935,87	-106,40	-154,92	-5,28	2,65
996,30	27,02	184,36	960,87	-115,22	-168,16	-5,85	2,68
1025,00	25,59	191,15	986,60	-122,79	-180,75	-7,54	3,48
1057,30	24,67	198,64	1015,85	-129,51	-193,98	-11,05	3,07
1086,40	23,71	205,98	1042,40	-133,97	-205,00	-15,55	3,25
1115,50	24,26	214,77	1069,00	-136,78	-215,17	-21,53	3,72
1144,40	24,96	223,04	1095,28	-137,88	-224,51	-29,08	3,65
1173,40	24,98	231,27	1121,58	-137,26	-232,81	-38,03	3,59
1202,50	24,99	237,59	1147,96	-135,09	-239,95	-48,02	2,75
1231,10	26,02	242,84	1173,78	-131,69	-246,06	-58,70	2,60
1260,50	27,99	247,17	1199,97	-126,94	-251,68	-70,80	2,84
1289,50	29,22	253,16	1225,44	-120,86	-256,37	-83,85	3,23
1318,10	30,82	259,25	1250,21	-113,28	-259,76	-97,73	3,61
1347,40	32,26	264,48	1275,18	-103,92	-261,91	-112,89	3,16
1375,90	33,09	269,46	1299,18	-93,48	-262,72	-128,25	2,96
1406,10	35,28	275,87	1324,16	-80,78	-261,90	-145,17	4,18
1434,70	37,97	281,77	1347,12	-66,87	-259,26	-162,01	4,64
1464,50	41,15	285,39	1370,10	-50,54	-254,79	-180,44	3,95
1493,60	44,46	286,63	1391,44	-33,12	-249,33	-199,45	3,52
1523,20	47,14	288,68	1412,08	-14,14	-242,89	-219,66	3,10
1552,00	49,58	289,45	1431,21	5,34	-235,86	-240,00	2,61
1579,40	50,29	289,58	1448,85	24,39	-228,85	-259,77	0,78
1608,50	52,87	290,60	1466,93	45,19	-221,02	-281,17	2,78
1635,50	56,12	293,11	1482,61	65,51	-212,83	-301,56	4,27

1666,80	58,75	295,36	1499,46	90,30	-201,99	-325,61	3,11
1697,70	61,78	296,31	1514,79	115,76	-190,30	-349,76	3,05
1727,80	64,19	296,84	1528,46	141,31	-178,30	-373,74	2,45
1756,80	66,98	300,04	1540,44	166,72	-165,72	-396,95	4,17
1785,80	69,81	300,61	1551,12	192,89	-152,11	-420,22	2,98
1814,90	72,19	302,59	1560,60	219,73	-137,69	-443,65	3,12
1843,80	75,32	302,49	1568,68	246,90	-122,77	-467,03	3,25
1872,70	79,01	303,73	1575,10	274,54	-107,38	-490,63	4,03
1901,80	82,29	306,09	1579,83	302,87	-90,95	-514,17	4,15
1931,00	85,83	307,36	1582,85	331,66	-73,58	-537,44	3,86
1959,10	87,67	308,65	1584,44	359,55	-56,31	-559,55	2,40
1989,70	87,64	308,83	1585,69	389,98	-37,18	-583,40	0,18
2018,60	88,35	309,14	1586,70	418,74	-19,01	-605,85	0,80
2047,80	90,06	312,55	1587,11	447,88	0,09	-627,93	3,92
2077,00	89,91	309,89	1587,12	477,04	19,32	-649,89	2,74
2106,10	89,98	309,70	1587,14	506,05	37,95	-672,25	0,21
2135,20	89,99	309,11	1587,15	535,05	56,42	-694,74	0,61
2164,50	89,97	308,98	1587,16	564,23	74,88	-717,49	0,13
2183,74	89,96	308,62	1587,18	583,39	86,94	-732,49	0,57
2189,00	93,50	308,60	1587,02	588,62	90,22	-736,59	20,21
2202,00	96,00	308,60	1585,94	601,51	98,30	-746,72	5,77
2220,90	95,04	309,25	1584,12	620,24	110,12	-761,35	1,84
2246,32	92,88	310,10	1582,37	645,52	126,31	-780,87	2,74
2274,90	91,19	310,51	1581,35	674,01	144,78	-802,65	1,83
2304,50	90,16	312,07	1581,00	703,57	164,31	-824,89	1,89
2333,10	87,94	313,84	1581,48	732,16	183,79	-845,82	2,98
2359,90	86,91	316,15	1582,68	758,92	202,72	-864,75	2,83
2390,70	87,56	319,92	1584,17	789,61	225,59	-885,31	3,72
2419,50	88,40	322,69	1585,18	818,17	248,06	-903,31	3,01
2446,90	88,94	326,08	1585,82	845,13	270,32	-919,26	3,76
2477,20	89,90	328,36	1586,13	874,65	295,79	-935,66	2,45
2506,10	89,89	331,68	1586,18	902,46	320,82	-950,10	3,45
2534,80	90,10	334,78	1586,18	929,59	346,44	-963,02	3,25
2563,70	90,30	336,14	1586,08	956,53	372,73	-975,03	1,43
2592,40	90,27	335,85	1585,94	983,18	398,95	-986,70	0,30
2621,30	90,31	334,79	1585,79	1010,15	425,21	-998,77	1,10
2649,10	90,34	334,47	1585,63	1036,20	450,33	-1010,68	0,35
2677,90	90,56	334,34	1585,41	1063,24	476,30	-1023,12	0,27
2707,50	89,92	333,42	1585,28	1091,11	502,88	-1036,15	1,14
2736,20	89,91	331,66	1585,33	1118,36	528,34	-1049,39	1,84
2765,20	91,15	330,75	1585,06	1146,09	553,75	-1063,35	1,59
2792,30	90,86	329,01	1584,58	1172,18	577,19	-1076,95	1,95
2822,70	90,70	327,48	1584,17	1201,67	603,04	-1092,95	1,52
2849,80	90,30	326,02	1583,93	1228,13	625,70	-1107,80	1,68
2878,90	90,31	324,19	1583,78	1256,70	649,56	-1124,45	1,89
2909,10	90,16	321,42	1583,65	1286,56	673,62	-1142,71	2,76
2937,90	90,14	321,37	1583,58	1315,14	696,13	-1160,68	0,06
2966,80	90,11	320,08	1583,51	1343,85	718,50	-1178,97	1,34
2995,60	89,43	320,51	1583,63	1372,49	740,65	-1197,37	0,84
3024,30	89,37	319,55	1583,93	1401,04	762,65	-1215,80	1,01
3053,40	89,78	317,98	1584,15	1430,05	784,53	-1234,98	1,67
3081,10	90,10	317,41	1584,18	1457,70	805,02	-1253,63	0,71
3111,10	90,10	318,66	1584,12	1487,63	827,32	-1273,69	1,25
3139,70	89,74	319,40	1584,16	1516,13	848,92	-1292,44	0,86

3168,20	89,78	319,75	1584,28	1544,51	870,61	-1310,92	0,37
3195,30	90,12	320,35	1584,31	1571,47	891,39	-1328,32	0,76
3224,60	90,49	319,92	1584,15	1600,61	913,88	-1347,10	0,58
3252,90	90,63	320,54	1583,87	1628,75	935,63	-1365,20	0,67
3283,30	90,16	319,82	1583,66	1658,99	958,97	-1384,67	0,85
3311,40	90,12	320,40	1583,60	1686,94	980,53	-1402,69	0,62
3342,10	90,15	319,94	1583,52	1717,48	1004,11	-1422,36	0,45
3371,10	90,09	320,45	1583,46	1746,32	1026,39	-1440,92	0,53
3399,80	89,92	320,15	1583,46	1774,86	1048,47	-1459,25	0,36
3428,70	89,40	320,22	1583,63	1803,60	1070,67	-1477,76	0,54
3456,30	89,93	320,74	1583,79	1831,04	1091,96	-1495,32	0,81
3485,60	90,27	320,84	1583,74	1860,14	1114,66	-1513,84	0,36
3514,70	90,64	318,68	1583,51	1889,11	1136,87	-1532,64	2,26
3545,00	89,81	316,46	1583,39	1919,35	1159,24	-1553,08	2,35
3574,00	89,72	315,26	1583,51	1948,34	1180,05	-1573,28	1,24
3603,00	89,93	315,64	1583,60	1977,33	1200,71	-1593,62	0,45
3632,00	89,95	315,98	1583,63	2006,32	1221,51	-1613,84	0,35
3661,30	89,91	315,69	1583,67	2035,61	1242,52	-1634,25	0,30
3690,10	90,13	314,98	1583,66	2064,40	1263,01	-1654,49	0,77
3719,10	90,09	314,77	1583,60	2093,40	1283,47	-1675,04	0,22
3748,30	89,67	314,96	1583,66	2122,60	1304,07	-1695,74	0,47
3758,50	89,76	313,76	1583,71	2132,80	1311,20	-1703,03	3,54
3787,10	89,76	313,15	1583,83	2161,40	1330,87	-1723,79	0,64
3816,10	89,89	313,34	1583,92	2190,39	1350,74	-1744,92	0,24
3845,00	90,06	313,41	1583,93	2219,29	1370,59	-1765,93	0,19
3874,00	90,05	312,21	1583,90	2248,28	1390,29	-1787,20	1,24
3903,20	89,90	313,11	1583,92	2277,47	1410,08	-1808,67	0,94
3932,20	90,07	313,11	1583,93	2306,46	1429,90	-1829,84	0,18
3957,50	88,36	312,47	1584,27	2331,75	1447,08	-1848,41	2,16
3978,30	90,18	311,21	1584,54	2352,53	1460,96	-1863,90	3,19
4007,80	91,14	309,39	1584,20	2381,96	1480,03	-1886,40	2,09
4036,40	89,95	306,47	1583,92	2410,38	1497,61	-1908,95	3,31
4077,40	89,72	305,26	1584,04	2450,94	1521,63	-1942,18	0,90
4106,50	89,99	304,26	1584,12	2479,65	1538,22	-1966,08	1,07
4135,10	90,31	304,14	1584,04	2507,81	1554,30	-1989,74	0,36
4164,50	90,39	303,17	1583,86	2536,71	1570,59	-2014,21	0,99
4193,60	90,47	305,55	1583,64	2565,38	1587,01	-2038,23	2,45
4222,40	89,69	306,23	1583,60	2593,87	1603,90	-2061,56	7,08
4251,10	89,92	307,14	1583,70	2622,32	1621,04	-2084,58	0,98
4280,40	90,05	307,02	1583,71	2651,39	1638,71	-2107,95	0,18
4309,60	90,13	306,00	1583,66	2680,33	1656,08	-2131,42	1,05
4338,80	90,74	305,04	1583,44	2709,19	1673,04	-2155,19	1,17
4367,70	89,85	304,37	1583,29	2737,69	1689,50	-2178,95	1,16
4396,70	89,62	304,22	1583,43	2766,26	1705,84	-2202,90	0,28
4425,80	90,09	303,96	1583,50	2794,90	1722,15	-2227,00	0,55
4454,90	90,10	304,30	1583,45	2823,55	1738,47	-2251,09	0,35
4484,30	89,92	301,90	1583,45	2852,39	1754,53	-2275,72	2,46
4513,10	90,12	305,14	1583,44	2880,69	1770,43	-2299,72	3,38
4542,10	89,17	307,17	1583,62	2909,40	1787,54	-2323,14	2,32
4571,30	89,35	306,54	1583,99	2938,36	1805,05	-2346,50	0,67
4600,30	89,04	311,89	1584,40	2967,23	1823,38	-2368,96	5,54
4629,50	89,44	315,38	1584,79	2996,42	1843,52	-2390,09	3,61
4658,90	88,71	318,69	1585,26	3025,78	1865,03	-2410,12	3,46
4687,70	89,46	322,46	1585,72	3054,39	1887,27	-2428,40	4,40

4717,00	90,21	326,53	1585,81	3083,22	1911,12	-2445,42	4,24
4746,00	90,40	329,05	1585,65	3111,41	1935,65	-2460,87	2,61
4775,10	89,98	330,83	1585,56	3139,42	1960,84	-2475,45	1,89
4804,00	90,05	333,48	1585,55	3166,91	1986,39	-2488,95	2,75
4833,00	90,00	337,80	1585,54	3193,91	2012,80	-2500,90	4,47
4862,10	89,90	339,98	1585,56	3220,35	2039,95	-2511,38	2,25
4891,00	89,62	343,28	1585,68	3246,00	2067,37	-2520,49	3,44
4920,20	89,78	346,34	1585,84	3271,14	2095,54	-2528,14	3,15
4949,40	89,79	347,86	1585,95	3295,66	2124,01	-2534,66	1,56
4978,60	90,59	349,22	1585,85	3319,78	2152,62	-2540,46	1,62
5007,70	90,15	351,26	1585,66	3343,32	2181,30	-2545,39	2,15
5036,60	90,60	352,19	1585,47	3366,25	2209,90	-2549,55	1,07
5066,20	90,63	354,01	1585,15	3389,29	2239,28	-2553,11	1,84
5095,20	90,33	354,57	1584,91	3411,49	2268,14	-2555,99	0,66
5124,30	90,69	353,56	1584,65	3433,83	2297,08	-2559,00	1,11
5153,50	89,85	349,77	1584,51	3457,01	2325,96	-2563,23	3,99
5183,10	89,46	348,04	1584,69	3481,35	2355,01	-2568,93	1,80
5211,90	89,30	343,77	1585,00	3505,86	2382,93	-2575,94	4,45
5241,20	89,84	342,65	1585,22	3531,49	2410,98	-2584,41	1,27
5270,60	88,85	340,53	1585,56	3557,59	2438,87	-2593,69	2,39
5299,60	88,93	337,33	1586,12	3583,93	2465,93	-2604,11	3,31
5328,80	90,45	334,17	1586,28	3611,09	2492,55	-2616,10	3,60
5357,80	90,45	330,66	1586,05	3638,64	2518,24	-2629,53	3,63
5387,00	90,87	327,44	1585,72	3666,86	2543,28	-2644,54	3,34
5414,60	91,42	325,26	1585,16	3693,84	2566,25	-2659,83	2,44
5441,50	91,43	322,60	1584,50	3720,34	2587,99	-2675,66	2,97
5468,60	90,35	322,34	1584,07	3747,16	2609,47	-2692,17	1,23
5497,50	90,35	321,53	1583,90	3775,80	2632,23	-2709,99	0,84
5524,30	91,01	319,84	1583,58	3802,43	2652,96	-2726,97	2,03
5552,30	90,09	317,55	1583,31	3830,34	2673,99	-2745,45	2,64
5581,30	90,14	315,08	1583,25	3859,32	2694,96	-2765,47	2,56
5608,40	90,16	312,70	1583,18	3886,41	2713,75	-2785,00	2,63
5635,90	90,08	310,59	1583,12	3913,88	2732,02	-2805,55	2,30
5663,70	91,87	309,04	1582,65	3941,60	2749,82	-2826,90	2,56
5691,50	91,87	308,25	1581,74	3969,25	2767,17	-2848,60	0,85
5718,90	91,89	308,77	1580,85	3996,50	2784,22	-2870,03	0,57
5746,20	93,47	308,86	1579,57	4023,65	2801,31	-2891,28	1,74
5757,00	93,47	308,86	1578,92	4034,38	2808,08	-2899,67	0,00

Table A-2: Well B1 survey

Measured Depth (m)	Inclination (deg)	Azimuth Grid (deg)	TVD (m)	Vertical Section (m)	NS Grid North (m)	EW Grid North (m)	DLS (deg/30 m)	Northing (m)	Easting (m)
0,00	0,00	0,00	0,00	0,00	-8,10	-0,80	0,00	7030824,70	615667,50
889,80	0,00	0,00	889,80	0,00	-8,10	-0,80	0,00	7030824,70	615667,50
893,22	0,67	152,22	893,22	0,02	-8,12	-0,79	5,88	7030824,68	615667,51
904,64	0,78	93,49	904,64	0,14	-8,18	-0,68	1,88	7030824,62	615667,62
914,06	1,01	63,33	914,06	0,22	-8,15	-0,54	1,64	7030824,65	615667,76
922,48	1,29	54,10	922,48	0,27	-8,06	-0,40	1,19	7030824,74	615667,90
942,00	1,58	205,20	941,99	0,40	-8,18	-0,34	4,27	7030824,63	615667,96
951,24	1,72	74,16	951,23	0,51	-8,25	-0,26	9,75	7030824,55	615668,04

1004,26	3,02	87,34	1004,21	1,93	-7,97	1,90	0,79	7030824,83	615670,20
1048,93	4,98	111,91	1048,77	4,59	-8,64	4,88	1,72	7030824,16	615673,18
1094,85	7,24	123,68	1094,43	9,33	-10,99	9,14	1,68	7030821,81	615677,43
1134,77	10,41	138,38	1133,87	15,41	-15,08	13,63	2,91	7030817,72	615681,92
1164,17	13,21	145,87	1162,65	21,30	-19,85	17,28	3,25	7030812,96	615685,57
1192,55	13,88	147,52	1190,24	27,73	-25,41	20,92	0,82	7030807,40	615689,22
1222,61	14,53	145,21	1219,38	34,87	-31,54	25,01	0,86	7030801,26	615693,30
1251,71	16,57	148,18	1247,42	42,40	-38,07	29,28	2,26	7030794,74	615697,57
1280,36	18,58	150,61	1274,73	50,64	-45,52	33,68	2,24	7030787,29	615701,97
1309,43	21,55	152,33	1302,03	60,03	-54,28	38,43	3,12	7030778,53	615706,72
1338,44	25,58	153,39	1328,62	70,85	-64,61	43,71	4,19	7030768,21	615712,00
1366,14	27,45	152,37	1353,40	82,39	-75,61	49,35	2,08	7030757,21	615717,64
1395,58	27,86	151,92	1379,48	95,20	-87,69	55,74	0,47	7030745,13	615724,02
1423,25	29,88	149,80	1403,71	107,83	-99,35	62,25	2,45	7030733,47	615730,53
1452,12	28,87	148,95	1428,87	121,33	-111,54	69,46	1,14	7030721,29	615737,74
1480,38	30,05	144,27	1453,47	134,76	-123,13	77,11	2,74	7030709,70	615745,39
1510,01	29,97	139,21	1479,14	149,35	-134,76	86,28	2,56	7030698,07	615754,56
1538,46	28,38	134,33	1503,98	163,15	-144,86	95,76	3,02	7030687,97	615764,04
1580,57	29,54	129,15	1540,83	183,53	-158,41	110,97	1,97	7030674,42	615779,25
1637,57	28,06	129,17	1590,78	210,96	-175,75	132,26	0,78	7030657,09	615800,53
1667,61	28,52	128,82	1617,23	225,18	-184,71	143,33	0,49	7030648,13	615811,60
1697,60	28,84	129,22	1643,54	239,55	-193,77	154,51	0,37	7030639,07	615822,77
1744,01	29,36	130,09	1684,09	262,11	-208,18	171,89	0,43	7030624,67	615840,15
1765,54	30,21	129,00	1702,78	272,79	-214,99	180,13	1,40	7030617,86	615848,39
1794,54	30,47	127,49	1727,81	287,41	-224,05	191,64	0,83	7030608,80	615859,89
1824,06	30,40	126,71	1753,26	302,31	-233,07	203,57	0,41	7030599,78	615871,82
1851,92	30,39	125,72	1777,29	316,34	-241,40	214,94	0,54	7030591,46	615883,19
1880,03	30,36	124,24	1801,54	330,45	-249,55	226,58	0,80	7030583,31	615894,83
1908,20	30,46	122,74	1825,84	344,56	-257,42	238,47	0,82	7030575,44	615906,72
1936,36	30,42	120,85	1850,12	358,61	-264,93	250,60	1,02	7030567,93	615918,84
1965,43	30,38	120,56	1875,19	373,04	-272,44	263,25	0,16	7030560,42	615931,49
1994,74	30,94	121,57	1900,40	387,73	-280,16	276,05	0,78	7030552,71	615944,28
2024,07	32,79	123,91	1925,31	403,01	-288,54	289,07	2,28	7030544,33	615957,30
2053,64	34,68	125,78	1949,90	419,31	-297,92	302,54	2,19	7030534,95	615970,77
2082,44	35,57	127,38	1973,46	435,81	-307,80	315,84	1,33	7030525,07	615984,07
2112,59	36,25	128,37	1997,88	453,45	-318,66	329,80	0,89	7030514,22	615998,02
2142,62	36,70	128,56	2022,02	471,28	-329,76	343,78	0,46	7030503,12	616012,00
2172,53	36,77	127,70	2046,00	489,13	-340,81	357,85	0,52	7030492,07	616026,06
2201,27	37,00	127,10	2068,98	506,33	-351,28	371,55	0,45	7030481,60	616039,76
2216,24	37,04	127,09	2080,94	515,31	-356,72	378,74	0,08	7030476,16	616046,95
2262,64	38,87	126,77	2117,52	543,74	-373,87	401,55	1,19	7030459,02	616069,76
2293,16	41,17	124,80	2140,89	563,25	-385,33	417,48	2,58	7030447,56	616085,68
2323,21	42,92	124,52	2163,21	583,22	-396,78	434,03	1,76	7030436,12	616102,23

2353,16	44,68	124,60	2184,82	603,78	-408,54	451,10	1,76	7030424,36	616119,29
2382,85	46,64	124,22	2205,57	624,84	-420,53	468,62	2,00	7030412,36	616136,81
2411,94	48,89	123,49	2225,12	646,17	-432,53	486,51	2,39	7030400,37	616154,69
2441,34	50,48	123,56	2244,15	668,35	-444,91	505,19	1,62	7030387,99	616173,37
2469,52	51,65	123,59	2261,85	690,04	-457,03	523,46	1,25	7030375,87	616191,63
2498,06	51,57	123,82	2279,58	712,19	-469,45	542,07	0,21	7030363,46	616210,24
2555,60	51,72	125,83	2315,29	756,97	-495,21	579,10	0,83	7030337,70	616247,27
2584,20	51,70	126,66	2333,01	779,31	-508,48	597,21	0,68	7030324,44	616265,36
2613,20	51,56	127,86	2351,01	801,98	-522,25	615,30	0,98	7030310,67	616283,46
2642,77	51,80	129,85	2369,35	825,14	-536,80	633,37	1,60	7030296,12	616301,52
2672,61	51,73	131,83	2387,81	848,58	-552,13	651,10	1,57	7030280,80	616319,24
2701,53	51,72	133,84	2405,73	871,27	-567,56	667,74	1,64	7030265,37	616335,89
2730,65	51,79	135,44	2423,76	894,11	-583,63	684,02	1,30	7030249,31	616352,15
2759,45	51,82	136,53	2441,57	916,69	-599,91	699,74	0,89	7030233,03	616367,88
2788,08	51,81	138,14	2459,27	939,09	-616,46	714,99	1,33	7030216,49	616383,12
2844,44	51,72	139,35	2494,15	983,03	-649,74	744,18	0,51	7030183,22	616412,31
2875,06	51,75	139,58	2513,11	1006,86	-668,01	759,81	0,18	7030164,95	616427,93
2905,02	51,61	139,17	2531,69	1030,16	-685,85	775,11	0,35	7030147,11	616443,23
2935,01	51,67	138,56	2550,30	1053,50	-703,56	790,58	0,48	7030129,41	616458,70
2963,98	51,63	137,42	2568,27	1076,09	-720,44	805,79	0,93	7030112,53	616473,90
2992,73	51,58	135,83	2586,13	1098,54	-736,82	821,26	1,30	7030096,16	616489,37
3021,60	51,61	134,60	2604,07	1121,12	-752,87	837,20	1,00	7030080,10	616505,30
3050,97	51,75	133,94	2622,28	1144,14	-768,96	853,70	0,55	7030064,02	616521,80
3078,28	53,52	133,58	2638,85	1165,84	-783,97	869,37	1,97	7030049,02	616537,47
3106,94	55,26	132,84	2655,54	1189,13	-799,92	886,36	1,93	7030033,07	616554,45
3136,27	56,70	131,65	2671,95	1213,44	-816,26	904,35	1,79	7030016,73	616572,44
3165,79	58,11	131,00	2687,85	1238,30	-832,68	923,03	1,54	7030000,31	616591,11
3224,78	60,90	130,01	2717,78	1289,12	-865,69	961,68	1,48	7029967,31	616629,75
3283,08	64,21	130,47	2744,65	1340,83	-899,11	1001,17	1,72	7029933,90	616669,23
3311,14	65,79	130,58	2756,51	1366,25	-915,63	1020,49	1,69	7029917,38	616688,55
3340,09	67,31	131,00	2768,03	1392,80	-932,98	1040,60	1,62	7029900,04	616708,66
3376,98	69,31	132,02	2781,66	1427,08	-955,70	1066,27	1,80	7029877,32	616734,32
3428,15	71,84	132,30	2798,68	1475,33	-988,09	1102,04	1,49	7029844,94	616770,08
3458,03	72,98	131,98	2807,71	1503,81	-1007,20	1123,16	1,18	7029825,84	616791,19
3495,42	73,88	132,17	2818,37	1539,65	-1031,22	1149,76	0,74	7029801,83	616817,78
3514,33	74,50	132,45	2823,52	1557,84	-1043,46	1163,21	1,07	7029789,58	616831,24
3543,84	75,72	133,05	2831,10	1586,36	-1062,82	1184,15	1,37	7029770,23	616852,17
3572,65	76,81	133,36	2837,94	1614,34	-1081,98	1204,55	1,18	7029751,07	616872,57
3601,03	77,57	133,48	2844,24	1642,00	-1101,00	1224,65	0,81	7029732,06	616892,66
3630,59	78,70	133,54	2850,31	1670,91	-1120,92	1245,63	1,15	7029712,15	616913,64
3660,38	78,76	133,85	2856,14	1700,11	-1141,10	1266,76	0,31	7029691,97	616934,76
3689,87	78,76	134,36	2861,88	1729,02	-1161,23	1287,53	0,51	7029671,84	616955,52
3718,60	79,28	134,43	2867,36	1757,19	-1180,96	1307,68	0,55	7029652,12	616975,67

3728,27	79,31	134,51	2869,15	1766,68	-1187,62	1314,46	0,26	7029645,46	616982,45
3733,37	79,31	134,53	2870,10	1771,69	-1191,13	1318,03	0,12	7029641,95	616986,02

Table A-3: Well B2 survey

Measured Depth (m)	Inclination (deg)	Azimuth Grid (deg)	TVD (m)	Vertical Section (m)	NS Grid North (m)	EW Grid North (m)	DLS (deg/30 m)	Northing (m)	Easting (m)
0,00	0,00	0,00	0,00	0,00	-5,30	-6,10	0,00	7030827,50	615662,20
889,80	0,00	0,00	889,80	0,00	-5,30	-6,10	0,00	7030827,50	615662,20
899,58	0,23	294,19	899,58	-0,01	-5,29	-6,12	0,71	7030827,51	615662,18
910,06	0,84	114,89	910,06	0,02	-5,32	-6,07	3,06	7030827,48	615662,23
947,09	1,54	111,77	947,08	0,41	-5,62	-5,36	0,57	7030827,19	615662,94
953,28	1,46	122,35	953,27	0,50	-5,69	-5,22	1,39	7030827,11	615663,08
1003,87	2,59	177,49	1003,83	2,05	-7,18	-4,62	1,26	7030825,63	615663,68
1031,75	3,09	189,83	1031,68	3,40	-8,55	-4,72	0,85	7030824,26	615663,58
1059,75	3,55	198,33	1059,63	4,90	-10,11	-5,12	0,72	7030822,69	615663,18
1089,57	5,08	201,17	1089,36	6,89	-12,22	-5,89	1,55	7030820,58	615662,41
1117,67	6,59	199,83	1117,32	9,41	-14,90	-6,89	1,62	7030817,91	615661,41
1146,79	7,74	198,76	1146,21	12,65	-18,33	-8,09	1,19	7030814,48	615660,22
1174,50	8,54	190,57	1173,64	16,28	-22,12	-9,06	1,52	7030810,69	615659,24
1204,64	10,17	178,74	1203,38	21,06	-26,98	-9,41	2,50	7030805,83	615658,89
1232,94	10,51	175,62	1231,22	26,12	-32,05	-9,16	0,69	7030800,76	615659,14
1261,80	11,75	175,93	1259,54	31,68	-37,60	-8,75	1,29	7030795,21	615659,55
1289,99	13,89	173,13	1287,03	37,93	-43,83	-8,14	2,37	7030788,98	615660,16
1319,05	15,56	172,67	1315,13	45,31	-51,16	-7,23	1,73	7030781,66	615661,07
1348,20	17,19	170,30	1343,10	53,53	-59,28	-6,01	1,81	7030773,53	615662,30
1366,89	18,22	167,78	1360,90	59,20	-64,86	-4,92	2,06	7030767,96	615663,38
1378,13	18,61	167,34	1371,57	62,74	-68,33	-4,16	1,11	7030764,49	615664,14
1405,10	19,77	163,60	1397,04	71,53	-76,90	-1,93	1,88	7030755,92	615666,38
1434,45	19,06	165,49	1424,72	81,19	-86,30	0,68	0,97	7030746,52	615668,98
1463,18	17,71	166,78	1451,98	90,20	-95,10	2,85	1,47	7030737,72	615671,15
1492,54	19,43	166,95	1479,81	99,50	-104,20	4,98	1,76	7030728,62	615673,27
1517,86	22,29	168,09	1503,47	108,48	-113,01	6,92	3,42	7030719,82	615675,22
1548,90	23,63	168,82	1532,05	120,56	-124,87	9,34	1,32	7030707,96	615677,64
1560,00	23,63	168,82	1542,22	125,00	-129,23	10,20	0,00	7030703,60	615678,50
1590,00	23,63	168,82	1569,71	137,00	-141,03	12,53	0,00	7030691,80	615680,83
1620,00	23,63	168,82	1597,19	149,00	-152,83	14,86	0,00	7030680,01	615683,16
1650,00	23,63	168,82	1624,67	161,00	-164,62	17,20	0,00	7030668,21	615685,49
1680,00	24,61	169,23	1652,06	173,24	-176,66	19,53	0,99	7030656,18	615687,83
1710,00	25,58	169,60	1679,22	185,94	-189,16	21,87	0,99	7030643,68	615690,16
1740,00	26,56	169,95	1706,17	199,11	-202,14	24,21	0,99	7030630,71	615692,50
1744,28	26,70	170,00	1710,00	201,03	-204,03	24,54	0,99	7030628,82	615692,83
1770,00	26,70	170,00	1732,97	212,57	-215,41	26,55	0,00	7030617,44	615694,84
1800,00	26,70	170,00	1759,78	226,04	-228,69	28,89	0,00	7030604,17	615697,18
1830,00	26,70	170,00	1786,58	239,51	-241,96	31,23	0,00	7030590,90	615699,52

1860,00	26,70	170,00	1813,38	252,98	-255,23	33,57	0,00	7030577,63	615701,86
1890,00	26,70	170,00	1840,18	266,44	-268,51	35,91	0,00	7030564,35	615704,20
1920,00	26,70	170,00	1866,98	279,91	-281,78	38,25	0,00	7030551,08	615706,54
1950,00	26,70	170,00	1893,78	293,38	-295,06	40,59	0,00	7030537,81	615708,88
1980,00	26,70	170,00	1920,58	306,84	-308,33	42,93	0,00	7030524,54	615711,22
2010,00	26,70	170,00	1947,38	320,31	-321,61	45,27	0,00	7030511,27	615713,56
2040,00	26,70	170,00	1974,18	333,78	-334,88	47,61	0,00	7030498,00	615715,90
2070,00	26,70	170,00	2000,99	347,24	-348,16	49,95	0,00	7030484,72	615718,24
2100,00	26,70	170,00	2027,79	360,71	-361,43	52,29	0,00	7030471,45	615720,58
2130,00	26,70	170,00	2054,59	374,18	-374,71	54,64	0,00	7030458,18	615722,92
2160,00	26,70	170,00	2081,39	387,64	-387,98	56,98	0,00	7030444,91	615725,26
2190,00	26,70	170,00	2108,19	401,11	-401,26	59,32	0,00	7030431,64	615727,60
2220,00	26,70	170,00	2134,99	414,58	-414,53	61,66	0,00	7030418,37	615729,94
2250,00	26,70	170,00	2161,79	428,04	-427,81	64,00	0,00	7030405,09	615732,28
2280,00	26,70	170,00	2188,59	441,51	-441,08	66,34	0,00	7030391,82	615734,62
2310,00	26,70	170,00	2215,39	454,98	-454,36	68,68	0,00	7030378,55	615736,96
2340,00	26,70	170,00	2242,20	468,44	-467,63	71,02	0,00	7030365,28	615739,30
2348,74	*26,70*	*170,00*	*2250,00*	*472,37*	*-471,50*	*71,70*	*0,00*	*7030361,41*	*615739,98*
2370,00	26,70	170,00	2269,00	481,91	-480,91	73,36	0,00	7030352,01	615741,64
2393,51	26,70	170,00	2290,00	492,47	-491,31	75,20	0,00	7030341,61	615743,48
2400,00	27,08	170,47	2295,79	495,40	-494,20	75,69	2,00	7030338,72	615743,97
2430,00	28,83	172,52	2322,29	509,46	-508,11	77,76	2,00	7030324,81	615746,05
2444,84	29,71	173,44	2335,23	516,71	-515,31	78,65	2,00	7030317,61	615746,93
2460,00	29,71	173,44	2348,40	524,22	-522,77	79,51	0,00	7030310,15	615747,79
2490,00	29,71	173,44	2374,46	539,09	-537,55	81,21	0,00	7030295,38	615749,49
2520,00	29,71	173,44	2400,51	553,96	-552,32	82,90	0,00	7030280,61	615751,18
2550,00	29,71	173,44	2426,57	568,82	-567,09	84,60	0,00	7030265,84	615752,88
2580,00	29,71	173,44	2452,62	583,69	-581,86	86,30	0,00	7030251,08	615754,58
2610,00	29,71	173,44	2478,68	598,56	-596,63	88,00	0,00	7030236,31	615756,28
2640,00	29,71	173,44	2504,74	613,43	-611,40	89,69	0,00	7030221,54	615757,97
2653,57	29,71	173,44	2516,53	620,15	-618,09	90,46	0,00	7030214,86	615758,74
2670,00	31,08	173,44	2530,69	628,46	-626,34	91,41	2,50	7030206,60	615759,69
2700,00	33,58	173,44	2556,04	644,50	-642,28	93,24	2,50	7030190,67	615761,52
2730,00	36,08	173,44	2580,66	661,63	-659,30	95,20	2,50	7030173,65	615763,48
2760,00	38,58	173,44	2604,52	679,82	-677,37	97,28	2,50	7030155,59	615765,55
2790,00	41,08	173,44	2627,55	699,03	-696,46	99,47	2,50	7030136,50	615767,75
2820,00	43,58	173,44	2649,73	719,23	-716,53	101,78	2,50	7030116,44	615770,06
2850,00	46,08	173,44	2671,01	740,37	-737,54	104,20	2,50	7030095,43	615772,47
2880,00	48,58	173,44	2691,34	762,43	-759,45	106,72	2,50	7030073,53	615774,99
2910,00	51,08	173,44	2710,69	785,35	-782,22	109,34	2,50	7030050,76	615777,61
2940,00	53,58	173,44	2729,02	809,09	-805,81	112,05	2,50	7030027,18	615780,32
2970,00	56,08	173,44	2746,30	833,61	-830,17	114,85	2,50	7030002,82	615783,12
3000,00	58,58	173,44	2762,49	858,85	-855,26	117,74	2,50	7029977,74	615786,01
3030,00	61,08	173,44	2777,57	884,79	-881,02	120,70	2,50	7029951,98	615788,97
3060,00	63,58	173,44	2791,50	911,35	-907,42	123,74	2,50	7029925,60	615792,01
3090,00	66,08	173,44	2804,25	938,49	-934,39	126,84	2,50	7029898,63	615795,11

3120,00	68,58	173,44	2815,82	966,17	-961,89	130,00	2,50	7029871,14	615798,27
3150,00	71,08	173,44	2826,16	994,32	-989,86	133,22	2,50	7029843,17	615801,49
3180,00	73,58	173,44	2835,27	1022,90	-1018,26	136,49	2,50	7029814,78	615804,76
3210,00	76,08	173,44	2843,12	1051,85	-1047,02	139,80	2,50	7029786,03	615808,07
3240,00	78,58	173,44	2849,69	1081,11	-1076,09	143,15	2,50	7029756,96	615811,41
3269,04	81,00	173,43	2854,84	1109,69	-1104,48	146,41	2,50	7029728,58	615814,68
3270,00	81,00	173,43	2854,99	1110,64	-1105,43	146,52	0,00	7029727,63	615814,79
3289,23	*81,00*	*173,43*	*2858,00*	*1129,63*	*-1124,29*	*148,69*	*0,00*	*7029708,77*	*615816,96*
3300,00	81,00	173,43	2859,68	1140,26	-1134,86	149,91	0,00	7029698,21	615818,17
3330,00	81,00	173,43	2864,38	1169,89	-1164,30	153,30	0,00	7029668,78	615821,56
3360,00	81,00	173,43	2869,07	1199,52	-1193,74	156,68	0,00	7029639,35	615824,95
3390,00	81,00	173,43	2873,76	1229,14	-1223,17	160,07	0,00	7029609,92	615828,33
3420,00	81,00	173,43	2878,46	1258,77	-1252,61	163,46	0,00	7029580,49	615831,72
3449,04	81,00	173,43	2883,00	1287,45	-1281,10	166,74	0,00	7029552,00	615835,00
3449,04	*81,00*	*173,43*	*2883,00*	*1287,45*	*-1281,11*	*166,74*	*0,00*	*7029552,00*	*615835,00*
3450,00	81,00	173,43	2883,15	1288,40	-1282,04	166,85	0,00	7029551,06	615835,11
3480,00	81,00	173,43	2887,84	1318,02	-1311,48	170,24	0,00	7029521,63	615838,50
3510,00	81,00	173,43	2892,54	1347,65	-1340,92	173,62	0,00	7029492,20	615841,88
3540,00	81,00	173,43	2897,23	1377,28	-1370,35	177,01	0,00	7029462,77	615845,27
3570,00	81,00	173,43	2901,92	1406,90	-1399,79	180,40	0,00	7029433,34	615848,66
3600,00	81,00	173,43	2906,62	1436,53	-1429,23	183,79	0,00	7029403,91	615852,04
3630,00	81,00	173,43	2911,31	1466,16	-1458,66	187,17	0,00	7029374,48	615855,43
3660,00	81,00	173,43	2916,00	1495,78	-1488,10	190,56	0,00	7029345,05	615858,82
3690,00	81,00	173,43	2920,69	1525,41	-1517,54	193,95	0,00	7029315,62	615862,20
3720,00	81,00	173,43	2925,39	1555,04	-1546,97	197,34	0,00	7029286,19	615865,59
3749,04	81,00	173,43	2929,93	1583,71	-1575,47	200,62	0,00	7029257,71	615868,87

Table A-4: Well B3 survey

Measured Depth (m)	Inclination (deg)	Azimuth Grid (deg)	TVD (m)	Vertical Section (m)	NS Grid North (m)	EW Grid North (m)	DLS (deg/30 m)	Northing (m)	Easting (m)
0,00	0,00	234,70	0,00	0,00	8,10	0,90	0,00	7030840,90	615669,20
889,80	*0,00*	*234,70*	*889,80*	*0,00*	*8,10*	*0,90*	*0,00*	*7030840,90*	*615669,20*
957,00	*0,00*	*234,70*	*957,00*	*0,00*	*8,10*	*0,90*	*0,00*	*7030840,90*	*615669,20*
1050,00	0,00	234,70	1050,00	0,00	8,10	0,90	0,00	7030840,90	615669,20
1374,15	16,21	234,70	1369,84	-40,34	-18,22	-36,27	1,50	7030814,59	615632,03
1565,93	*16,21*	*234,70*	*1554,00*	*-87,75*	*-49,16*	*-79,97*	*0,00*	*7030783,66*	*615588,35*
1853,36	16,21	234,70	1830,00	-158,80	-95,52	-145,45	0,00	7030737,30	615522,88
2269,94	9,41	129,00	2240,00	-187,21	-151,16	-166,68	1,50	7030681,67	615501,66
2280,08	*9,41*	*129,00*	*2250,00*	*-186,08*	*-152,21*	*-165,39*	*0,00*	*7030680,63*	*615502,95*
2290,21	9,41	129,00	2260,00	-184,94	-153,25	-164,10	0,00	7030679,59	615504,24
2310,00	10,52	121,16	2279,49	-182,42	-155,20	-161,30	2,65	7030677,63	615507,04
2340,00	12,47	112,15	2308,89	-177,47	-157,84	-155,95	2,65	7030675,00	615512,38
2370,00	14,65	105,66	2338,05	-171,17	-160,09	-149,30	2,65	7030672,75	615519,04
2400,00	16,95	100,86	2366,92	-163,54	-161,93	-141,35	2,65	7030670,90	615526,98

2430,00	19,35	97,19	2395,43	-154,59	-163,38	-132,12	2,65	7030669,46	615536,21
2460,00	21,80	94,32	2423,51	-144,33	-164,42	-121,64	2,65	7030668,42	615546,69
2490,00	24,29	92,00	2451,12	-132,80	-165,06	-109,92	2,65	7030667,78	615558,41
2520,00	26,81	90,10	2478,18	-120,01	-165,29	-96,98	2,65	7030667,55	615571,34
2550,00	29,35	88,50	2504,65	-105,99	-165,10	-82,87	2,65	7030667,74	615585,45
2580,00	31,91	87,13	2530,46	-90,78	-164,51	-67,60	2,65	7030668,33	615600,72
2610,00	34,48	85,95	2555,57	-74,40	-163,52	-51,21	2,65	7030669,32	615617,11
2640,00	37,05	84,91	2579,91	-56,90	-162,11	-33,73	2,65	7030670,72	615634,58
2670,00	39,64	83,99	2603,43	-38,30	-160,31	-15,21	2,65	7030672,53	615653,10
2700,00	42,24	83,17	2626,09	-18,64	-158,11	4,33	2,65	7030674,73	615672,62
2730,00	44,84	82,42	2647,84	2,02	-155,51	24,83	2,65	7030677,32	615693,12
2760,00	47,44	81,74	2668,62	23,65	-152,53	46,25	2,65	7030680,30	615714,54
2790,00	50,05	81,11	2688,41	46,19	-149,17	68,55	2,65	7030683,67	615736,83
2820,00	52,66	80,53	2707,14	69,61	-145,43	91,67	2,65	7030687,41	615759,95
2828,31	53,38	80,38	2712,14	76,25	-144,33	98,22	2,65	7030688,51	615766,50
2831,34	53,38	80,38	2713,95	78,68	-143,92	100,62	0,00	7030688,91	615768,90
2850,00	55,03	80,38	2724,86	93,81	-141,39	115,54	2,65	7030691,44	615783,81
2880,00	57,68	80,38	2741,48	118,76	-137,22	140,16	2,65	7030695,61	615808,43
2910,00	60,33	80,38	2756,92	144,46	-132,92	165,52	2,65	7030699,91	615833,78
2940,00	62,98	80,38	2771,16	170,85	-128,51	191,55	2,65	7030704,32	615859,80
2970,00	65,63	80,38	2784,17	197,86	-123,99	218,20	2,65	7030708,84	615886,45
3000,00	68,28	80,38	2795,91	225,45	-119,38	245,41	2,65	7030713,45	615913,65
3030,00	70,93	80,38	2806,37	253,55	-114,68	273,13	2,65	7030718,15	615941,37
3060,00	73,58	80,38	2815,51	282,10	-109,91	301,30	2,65	7030722,92	615969,53
3090,00	76,23	80,38	2823,32	311,05	-105,07	329,86	2,65	7030727,76	615998,08
3120,00	78,88	80,38	2829,78	340,32	-100,17	358,74	2,65	7030732,65	616026,95
3143,98	81,00	80,38	2833,97	363,92	-96,23	382,02	2,65	7030736,60	616050,23
3144,17	*81,00*	*80,38*	*2834,00*	*364,11*	*-96,19*	*382,20*	*0,00*	*7030736,63*	*616050,41*
3150,00	81,00	80,38	2834,91	369,86	-95,23	387,88	0,00	7030737,59	616056,09
3180,00	81,00	80,38	2839,60	399,47	-90,28	417,09	0,00	7030742,54	616085,29
3210,00	81,00	80,38	2844,30	429,09	-85,33	446,31	0,00	7030747,49	616114,50
3240,00	81,00	80,38	2848,99	458,70	-80,38	475,52	0,00	7030752,44	616143,71
3270,00	81,00	80,38	2853,68	488,31	-75,43	504,74	0,00	7030757,39	616172,92
3300,00	81,00	80,38	2858,38	517,92	-70,47	533,95	0,00	7030762,34	616202,12
3303,98	81,00	80,38	2859,00	521,85	-69,82	537,83	0,00	7030763,00	616206,00
3303,99	*81,00*	*80,38*	*2859,00*	*521,86*	*-69,82*	*537,83*	*0,00*	*7030763,00*	*616206,01*
3330,00	81,00	80,38	2863,07	547,54	-65,52	563,16	0,00	7030767,29	616231,33
3360,00	81,00	80,38	2867,76	577,15	-60,57	592,38	0,00	7030772,24	616260,54
3390,00	81,00	80,38	2872,46	606,76	-55,62	621,59	0,00	7030777,19	616289,74
3420,00	81,00	80,38	2877,15	636,37	-50,67	650,80	0,00	7030782,14	616318,95
3450,00	81,00	80,38	2881,84	665,99	-45,72	680,02	0,00	7030787,10	616348,16
3480,00	81,00	80,38	2886,54	695,60	-40,76	709,23	0,00	7030792,05	616377,37
3510,00	81,00	80,38	2891,23	725,21	-35,81	738,45	0,00	7030797,00	616406,57
3540,00	81,00	80,38	2895,92	754,82	-30,86	767,66	0,00	7030801,95	616435,78
3570,00	81,00	80,38	2900,61	784,44	-25,91	796,87	0,00	7030806,90	616464,99
3600,00	81,00	80,38	2905,31	814,05	-20,96	826,09	0,00	7030811,85	616494,19

3603,98	81,00	80,38	2905,93	817,98	-20,30	829,97	0,00	7030812,50	616498,07

Figure A-11: B1 early stage well diagram

AHBDF Top (m)	TVBDF (m)	Dev	Schematic	Description	Max OD, inch	ID, inch	Drift, inch
				Tubing Details — *Casing / Liner Details*			
886,0	886	0	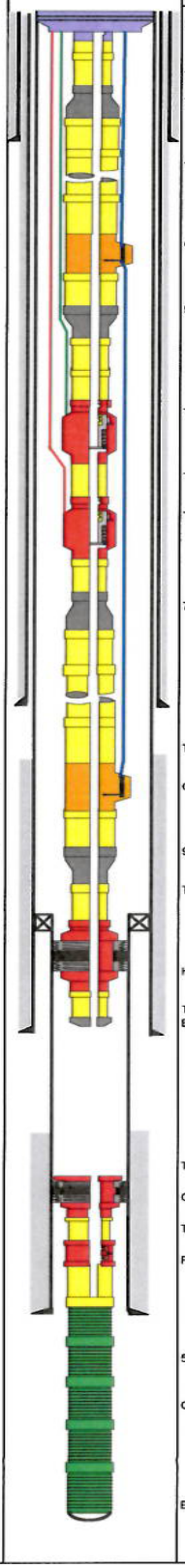	Landing point for FMC Tubing Hanger		6,059	6,049
888,0	888	0		Tubing: 7" 32 lb/ft Vam Top HC box x pin	7,070	6,094	6,000
908,6	909	1		7" 32 lb/ft Vam Top HC Box x 9 5/8" 53.5 lb/ft Vam Top ND Pin Xover	10,519	6,083	6,000
				30" Conductor shoe		28,000	
				Tubing: 9 5/8" 53.5 lb/ft Vam Top ND	9,741	8,535	8,379
				20" 129lb/ft X-65 S60D Surface Casing		18,750	
1581,0	1561	24		Gauge Mandrel 9 5/8" 53.5 lb/ft Vam Top ND box x pin	11,140	8,525	8,379
1599,0	1577	24		9 5/8" 53.5 lb/ft Vam Top ND Box x 7" 32 lb/ft Vam Top HC Pin Xover	10,519	6,083	6,000
				13 5/8" 88,2lb/ft P110 Production Casing		12,375	12,188
1626,0	1602	25		Tubing Retrievable Subsurface Safety Valve - Yellow C/L	9,200	5,953	
				Tubing: 7" 32 lb/ft Vam Top HC Box x Pin	7,070	6,094	6,000
1646,0	1620	26		Tubing Retrievable Subsurface Safety Valve - Red C/L	9,200	5,875	
1667,0	1639	26		7" 32 lb/ft Vam Top HC Box x 9 5/8" 53.5 lb/ft Vam Top ND Pin Xover	10,519	6,083	6,000
				20" shoe @ ca. 1632.1m		12,375	12,188
				Tubing: 9 5/8" 53.5 lb/ft Vam Top ND Box x Pin	9,741	8,535	8,379
2278,0	2138	39		Gauge Mandrel 9 5/8" 53.5 lb/ft Vam Top ND Box x Pin	11,140	8,525	8,379
				13 5/8" 88,2lb/ft P110 Production Casing		12,375	12,188
2301,8	2157	39		9 5/8" 53.5 lb/ft Vam Top ND Box x 7" 32 lb/ft Vam Top HC Pin Xover Assembly	10,519	6,083	6,000
				Tubing: 7" 32 lb/ft Vam Top HC box x pin	7,070	6,094	6,000
2321,8	2172	39		*9 5/8" top PBR as tagged by PBR dress mill* *9 5/8" top ZX Packer*			
2371,8	2211	39		HHC 9 5/8" x7" Hydrostatic Set Packer - Piptag Installed	8,350	6,000	5,969
2401,0	2234	39		Tubing: 7" 32 lb/ft Vam Top HC Box x Pin Bottom of Bell Guide WEG	7,070 8,350	6,094 5,975	6,000 5,969
2421,8	2250	39		*13 5/8" 88,2# Casing shoe*		12,375	12,188
				9-5/8" 53.5# M110 SM13Cr Liner		8,535	8,379
				Top of Straddle Entry Guide - Not latched	8,120	4,790	4,767
3817,5	2872	81		Gravel Pack Packer. Piptag Installed	8,313	6,000	5,937
				Tubing: 7" 32 lb/ft Vam Top HC Box x Pin	7,070	6,094	6,000
3852,5	2877	81		FIV	8,000	4,600	4,545
3877,5	2881	81		*9 5/8" 53.5# P110 13Cr shoe*		8,535	8,379
				5-1/2" Wire Wrap Sand Screens			
				Open Hole Gravel Pack Screens with 16/30 Carbolite Pack	7,770	6,094	5,969
				8-1/2" Open Hole Section		8,500	
4177,5	2928	81		Bottom of GPV 6 5/8" Vam Top HC Shoe	7,745		

Figure A-12: B2 early stage well diagram

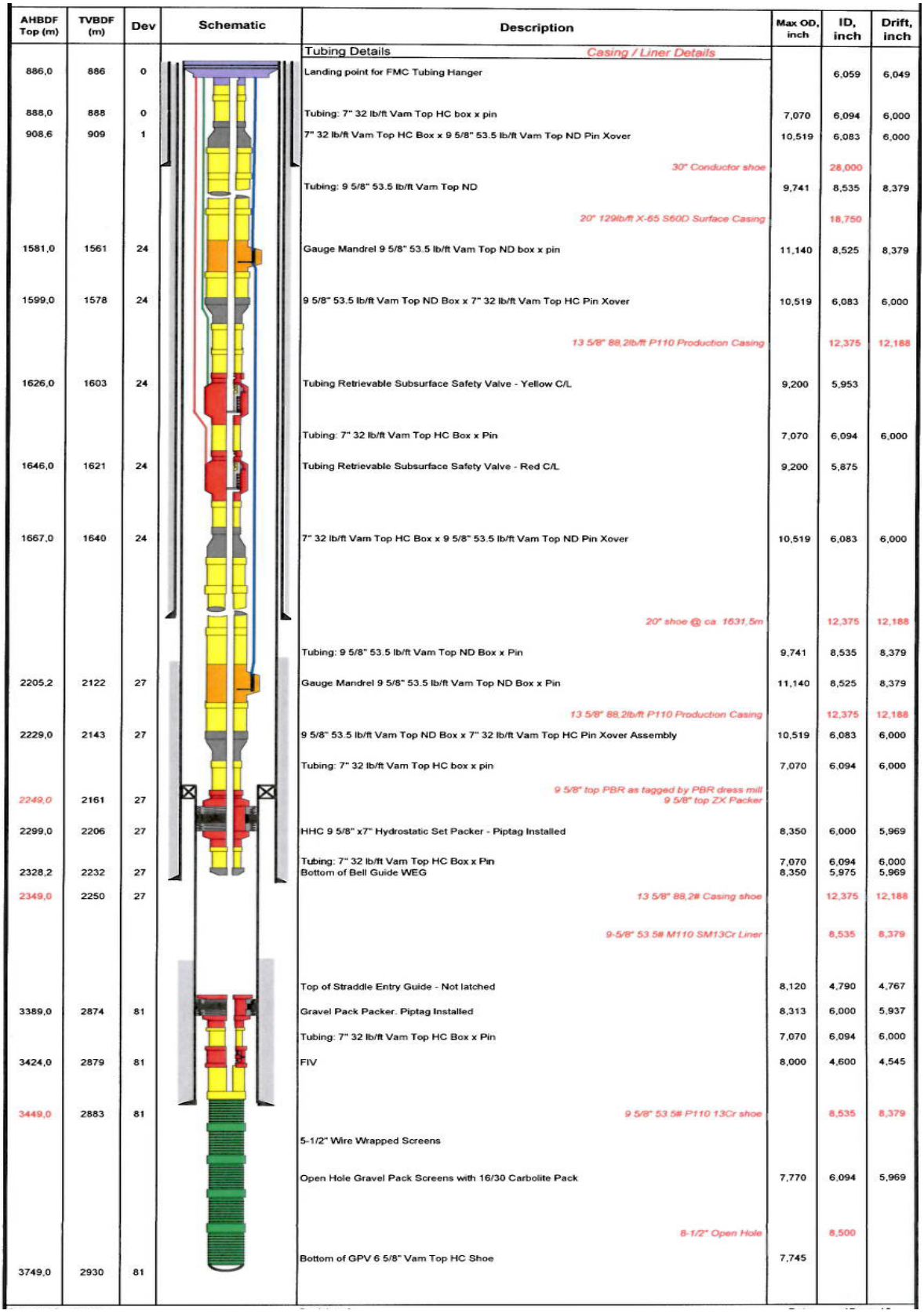

AHBDF Top (m)	TVBDF (m)	Dev	Description	Max OD, inch	ID, inch	Drift, inch
			Tubing Details / *Casing / Liner Details*			
886,0	886	0	Landing point for FMC Tubing Hanger		6,059	6,049
888,0	888	0	Tubing: 7" 32 lb/ft Vam Top HC box x pin	7,070	6,094	6,000
908,6	909	1	7" 32 lb/ft Vam Top HC Box x 9 5/8" 53.5 lb/ft Vam Top ND Pin Xover	10,519	6,083	6,000
			30" Conductor shoe		28,000	
			Tubing: 9 5/8" 53.5 lb/ft Vam Top ND	9,741	8,535	8,379
			20" 129lb/ft X-65 S60D Surface Casing		18,750	
1581,0	1561	24	Gauge Mandrel 9 5/8" 53.5 lb/ft Vam Top ND box x pin	11,140	8,525	8,379
1599,0	1578	24	9 5/8" 53.5 lb/ft Vam Top ND Box x 7" 32 lb/ft Vam Top HC Pin Xover	10,519	6,083	6,000
			13 5/8" 88,2lb/ft P110 Production Casing		12,375	12,188
1626,0	1603	24	Tubing Retrievable Subsurface Safety Valve - Yellow C/L	9,200	5,953	
			Tubing: 7" 32 lb/ft Vam Top HC Box x Pin	7,070	6,094	6,000
1646,0	1621	24	Tubing Retrievable Subsurface Safety Valve - Red C/L	9,200	5,875	
1667,0	1640	24	7" 32 lb/ft Vam Top HC Box x 9 5/8" 53.5 lb/ft Vam Top ND Pin Xover	10,519	6,083	6,000
			20" shoe @ ca. 1631,5m		12,375	12,188
			Tubing: 9 5/8" 53.5 lb/ft Vam Top ND Box x Pin	9,741	8,535	8,379
2205,2	2122	27	Gauge Mandrel 9 5/8" 53.5 lb/ft Vam Top ND Box x Pin	11,140	8,525	8,379
			13 5/8" 88,2lb/ft P110 Production Casing		12,375	12,188
2229,0	2143	27	9 5/8" 53.5 lb/ft Vam Top ND Box x 7" 32 lb/ft Vam Top HC Pin Xover Assembly	10,519	6,083	6,000
			Tubing: 7" 32 lb/ft Vam Top HC box x pin	7,070	6,094	6,000
2249,0	2161	27	*9 5/8" top PBR as tagged by PBR dress mill* *9 5/8" top ZX Packer*			
2299,0	2206	27	HHC 9 5/8" x7" Hydrostatic Set Packer - Piptag Installed	8,350	6,000	5,969
			Tubing: 7" 32 lb/ft Vam Top HC Box x Pin	7,070	6,094	6,000
2328,2	2232	27	Bottom of Bell Guide WEG	8,350	5,975	5,969
2349,0	2250	27	*13 5/8" 88,2# Casing shoe*		12,375	12,188
			9-5/8" 53.5# M110 SM13Cr Liner		8,535	8,379
			Top of Straddle Entry Guide - Not latched	8,120	4,790	4,767
3389,0	2874	81	Gravel Pack Packer. Piptag Installed	8,313	6,000	5,937
			Tubing: 7" 32 lb/ft Vam Top HC Box x Pin	7,070	6,094	6,000
3424,0	2879	81	FIV	8,000	4,600	4,545
3449,0	2883	81	*9 5/8" 53.5# P110 13Cr shoe*		8,535	8,379
			5-1/2" Wire Wrapped Screens			
			Open Hole Gravel Pack Screens with 16/30 Carbolite Pack	7,770	6,094	5,969
			8-1/2" Open Hole		8,500	
3749,0	2930	81	Bottom of GPV 6 5/8" Vam Top HC Shoe	7,745		

Figure A-11: B3 early stage well diagram

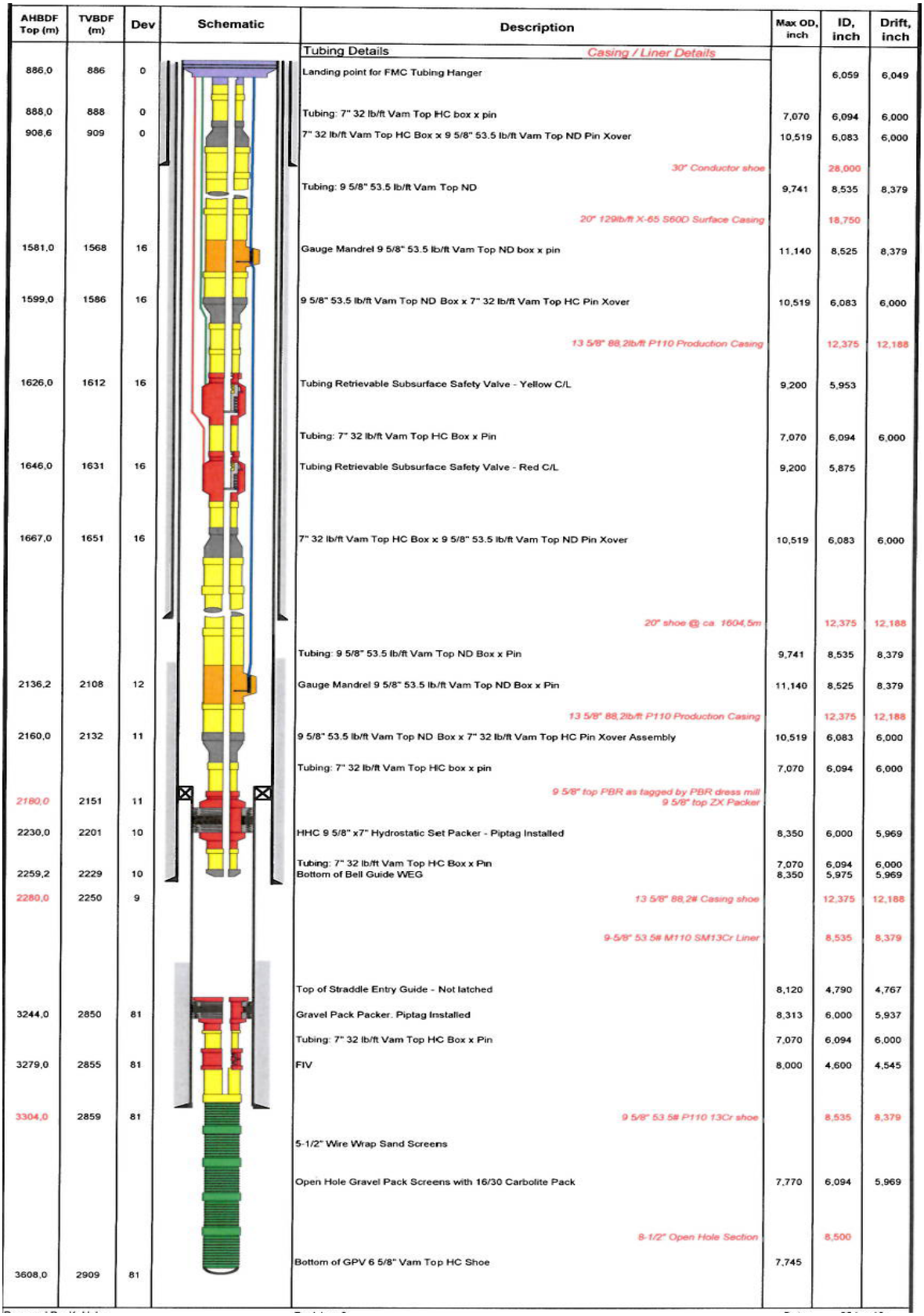

AHBDF Top (m)	TVBDF (m)	Dev	Description	Max OD, inch	ID, inch	Drift, inch
			Tubing Details / *Casing / Liner Details*			
886,0	886	0	Landing point for FMC Tubing Hanger		6,059	6,049
888,0	888	0	Tubing: 7" 32 lb/ft Vam Top HC box x pin	7,070	6,094	6,000
908,6	909	0	7" 32 lb/ft Vam Top HC Box x 9 5/8" 53.5 lb/ft Vam Top ND Pin Xover	10,519	6,083	6,000
			30" Conductor shoe		28,000	
			Tubing: 9 5/8" 53.5 lb/ft Vam Top ND	9,741	8,535	8,379
			20" 129lb/ft X-65 S60D Surface Casing		18,750	
1581,0	1568	16	Gauge Mandrel 9 5/8" 53.5 lb/ft Vam Top ND box x pin	11,140	8,525	8,379
1599,0	1586	16	9 5/8" 53.5 lb/ft Vam Top ND Box x 7" 32 lb/ft Vam Top HC Pin Xover	10,519	6,083	6,000
			13 5/8" 88,2lb/ft P110 Production Casing		12,375	12,188
1626,0	1612	16	Tubing Retrievable Subsurface Safety Valve - Yellow C/L	9,200	5,953	
			Tubing: 7" 32 lb/ft Vam Top HC Box x Pin	7,070	6,094	6,000
1646,0	1631	16	Tubing Retrievable Subsurface Safety Valve - Red C/L	9,200	5,875	
1667,0	1651	16	7" 32 lb/ft Vam Top HC Box x 9 5/8" 53.5 lb/ft Vam Top ND Pin Xover	10,519	6,083	6,000
			20" shoe @ ca. 1604,5m		12,375	12,188
			Tubing: 9 5/8" 53.5 lb/ft Vam Top ND Box x Pin	9,741	8,535	8,379
2136,2	2108	12	Gauge Mandrel 9 5/8" 53.5 lb/ft Vam Top ND Box x Pin	11,140	8,525	8,379
			13 5/8" 88,2lb/ft P110 Production Casing		12,375	12,188
2160,0	2132	11	9 5/8" 53.5 lb/ft Vam Top ND Box x 7" 32 lb/ft Vam Top HC Pin Xover Assembly	10,519	6,083	6,000
			Tubing: 7" 32 lb/ft Vam Top HC box x pin	7,070	6,094	6,000
2180,0	2151	11	*9 5/8" top PBR as tagged by PBR dress mill* *9 5/8" top ZX Packer*			
2230,0	2201	10	HHC 9 5/8" x7" Hydrostatic Set Packer - Piptag Installed	8,350	6,000	5,969
2259,2	2229	10	Tubing: 7" 32 lb/ft Vam Top HC Box x Pin Bottom of Bell Guide WEG	7,070 8,350	6,094 5,975	6,000 5,969
2280,0	2250	9	*13 5/8" 88,2# Casing shoe*		12,375	12,188
			9-5/8" 53.5# M110 SM13Cr Liner		8,535	8,379
			Top of Straddle Entry Guide - Not latched	8,120	4,790	4,767
3244,0	2850	81	Gravel Pack Packer. Piptag Installed	8,313	6,000	5,937
			Tubing: 7" 32 lb/ft Vam Top HC Box x Pin	7,070	6,094	6,000
3279,0	2855	81	FIV	8,000	4,600	4,545
3304,0	2859	81	*9 5/8" 53.5# P110 13Cr shoe*		8,535	8,379
			5-1/2" Wire Wrap Sand Screens			
			Open Hole Gravel Pack Screens with 16/30 Carbolite Pack	7,770	6,094	5,969
			8-1/2" Open Hole Section		8,500	
3608,0	2909	81	Bottom of GPV 6 5/8" Vam Top HC Shoe	7,745		